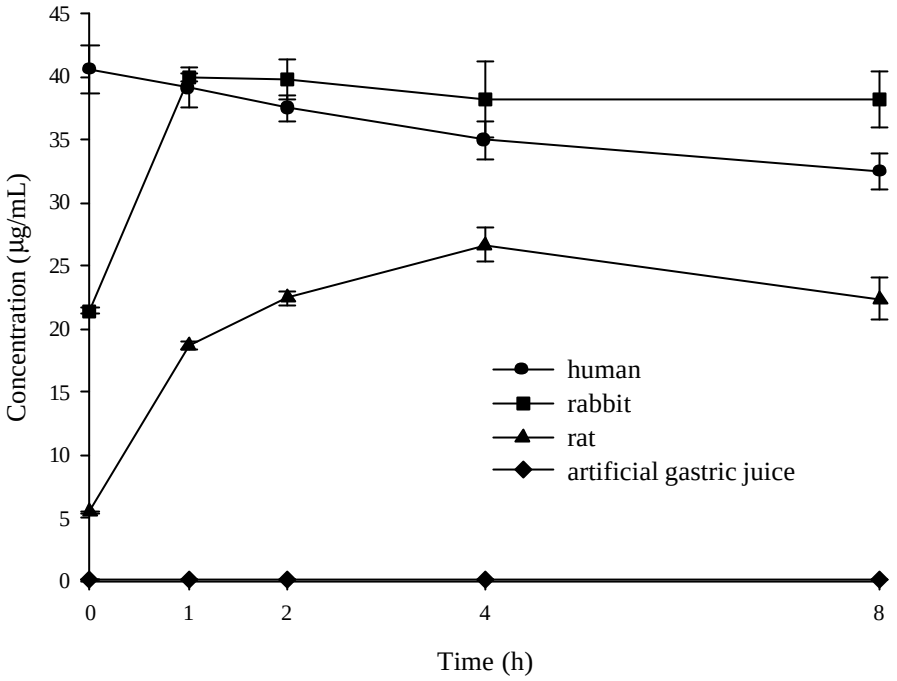

Fig. 1. Mean (± S.D.) concentration-time profiles of hesperetin after incubation of hesperidin with human, rabbit, rat feces and artificial gastric juice (n=3).

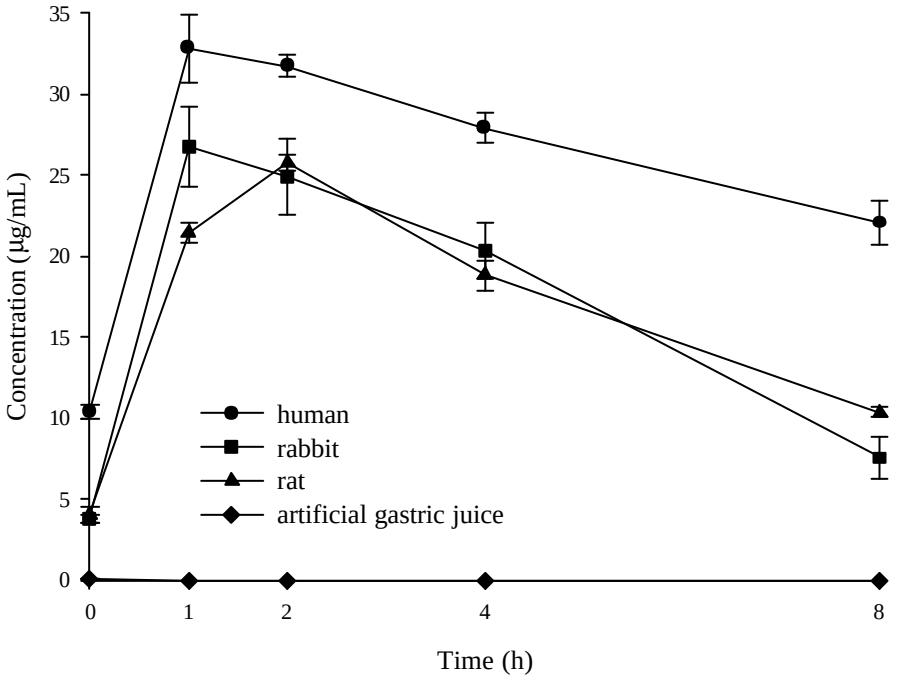

Fig. 2. Mean (± S.D.) concentration-time profiles of naringenin after incubation of naringin with human, rabbit, rat feces and artificial gastric juice (n=3).

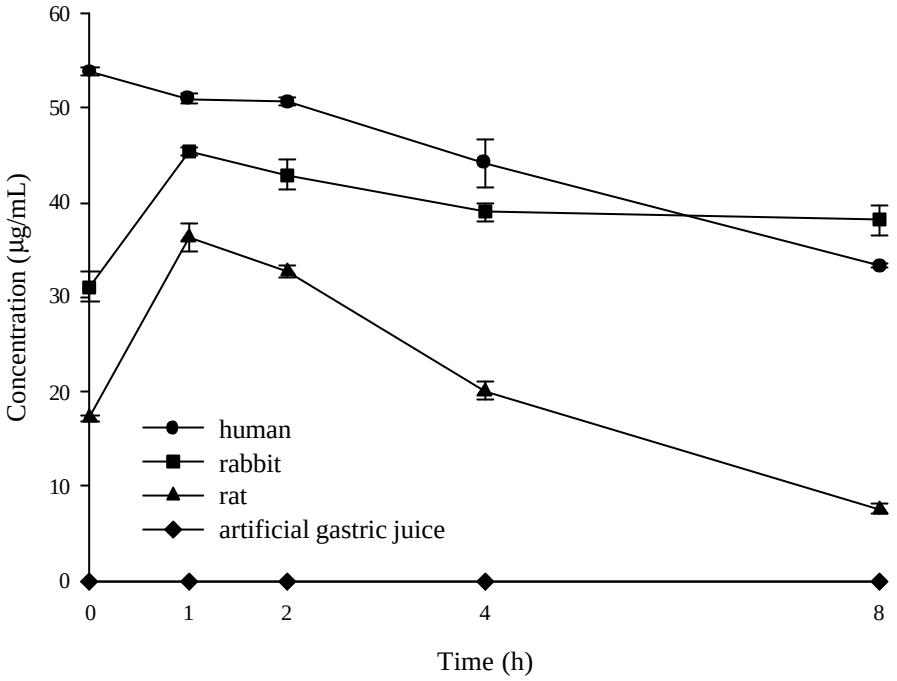

Fig. 3. Mean (± S.D.) concentration-time profiles of quercetin after incubation of rutin with human, rabbit, rat feces and artificial gastric juice (n=3).

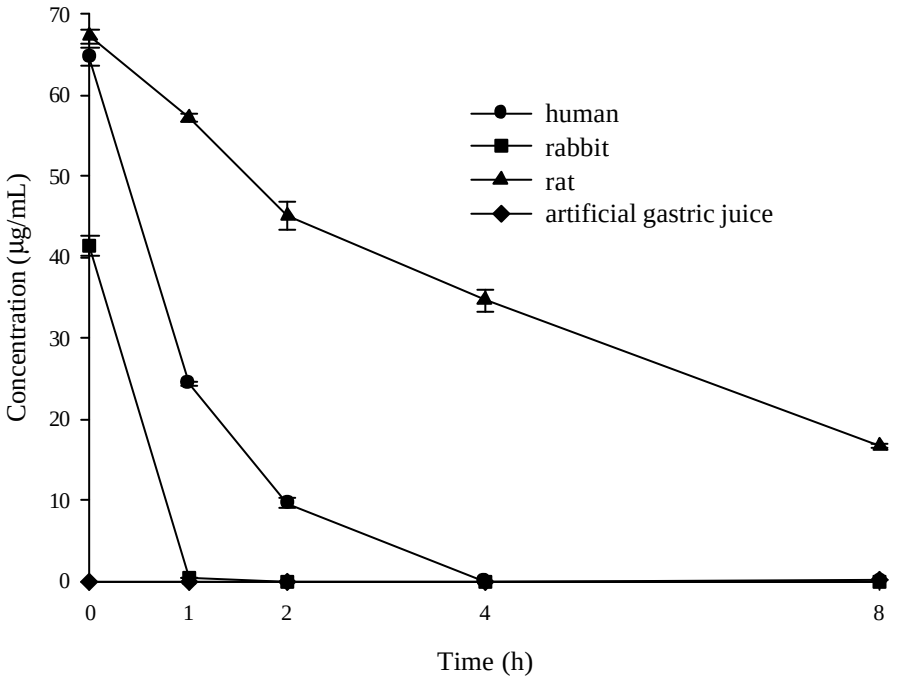

Fig. 4. Mean (± S.D.) concentration-time profiles of neophellamuretin after incubation of phellamurin with human, rabbit, rat feces and artificial gastric juice (n=3).

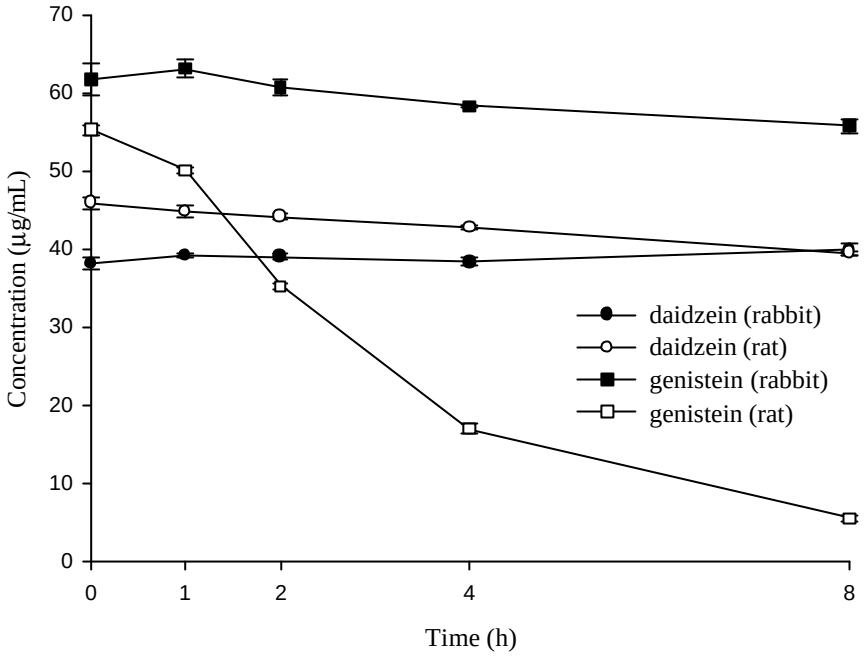

Fig. 5. Mean (± S.D.) concentration-time profiles of daidzein and genistein after incubation of daidzin and genistin with rabbit and rat feces (n=3).

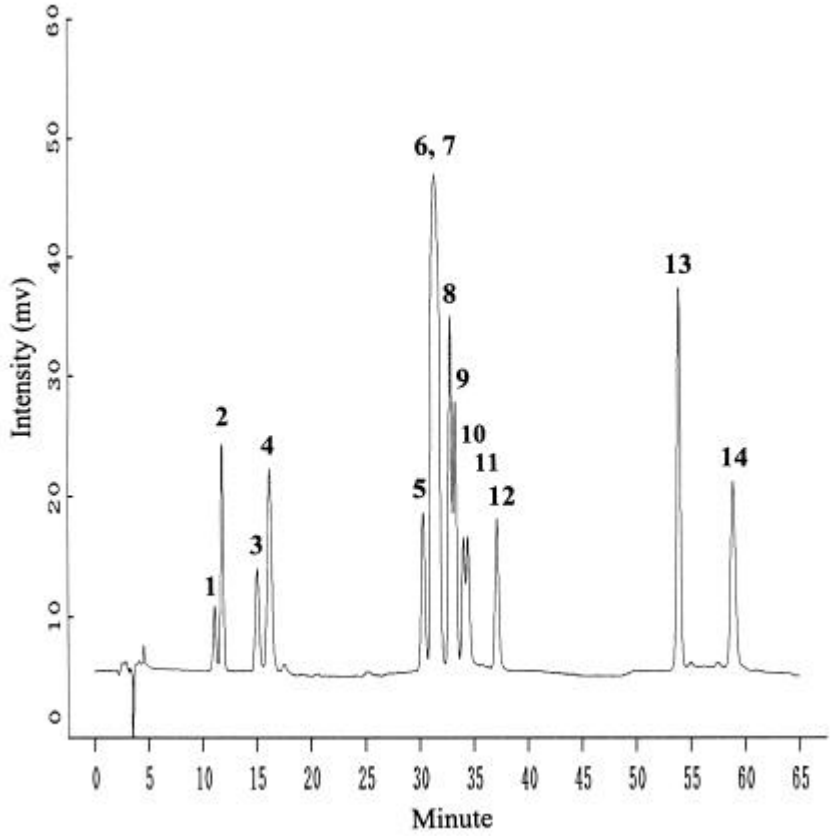

Fig. 6. HPLC chromatogram of flavonoid standards, **1**: morin; **2**: daidzein; **3**: luteolin; **4**: quercetin; **5**: genistein; **6**: naringenin; **7**: apigenin; **8**: hesperetin; **9**: diosmetin; **10**: kaempferol; **11**: baicalein; **12**: 5, 7-dimethoxycoumarin (I.S.); **13**: neophellamuretin; **14**: wogonin.

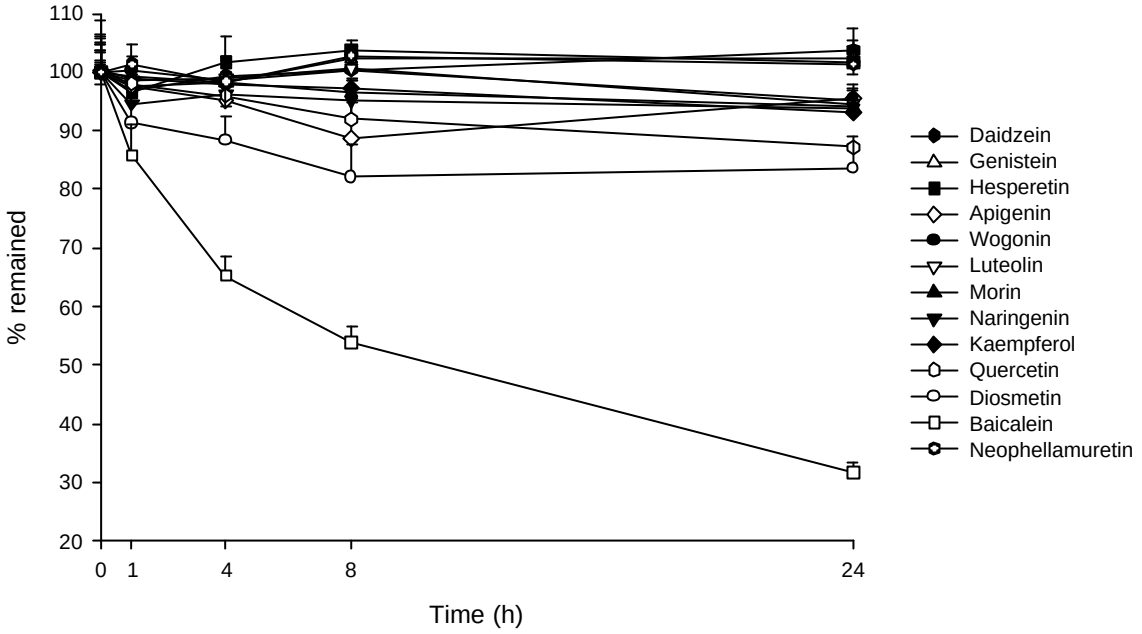

Fig. 7. Degradation of flavonoid aglycones by artificial intestinal juice (Mean ± S.D. for each time point, n=3).

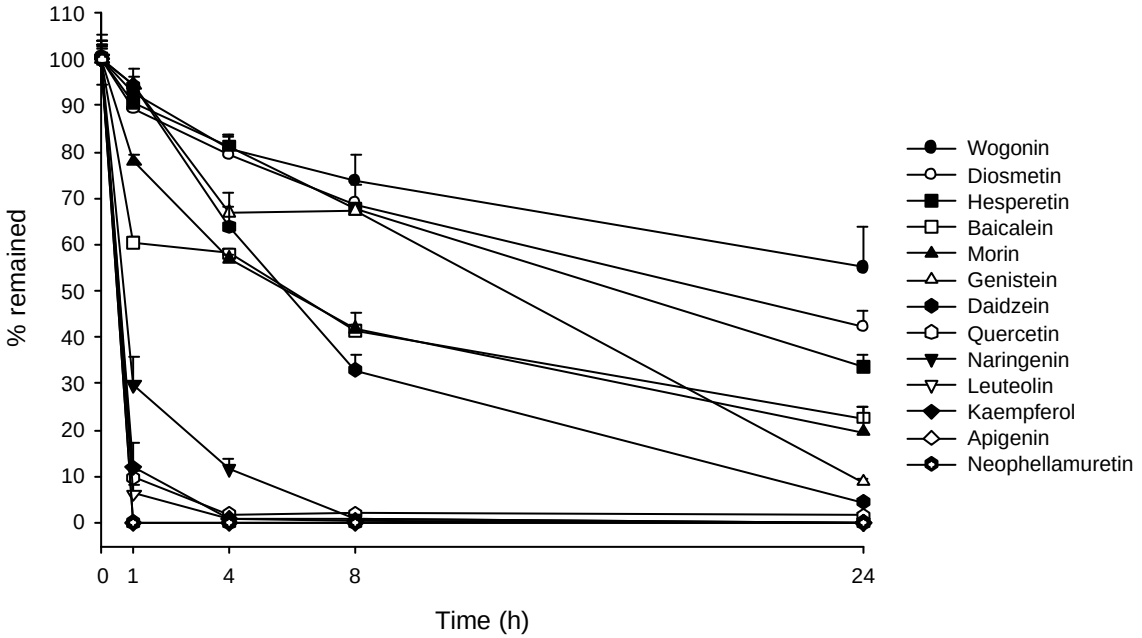

Fig. 8. Degradation of flavonoid aglycones by rabbit fecal flora (Mean ± S.D. for each time point, n=3).

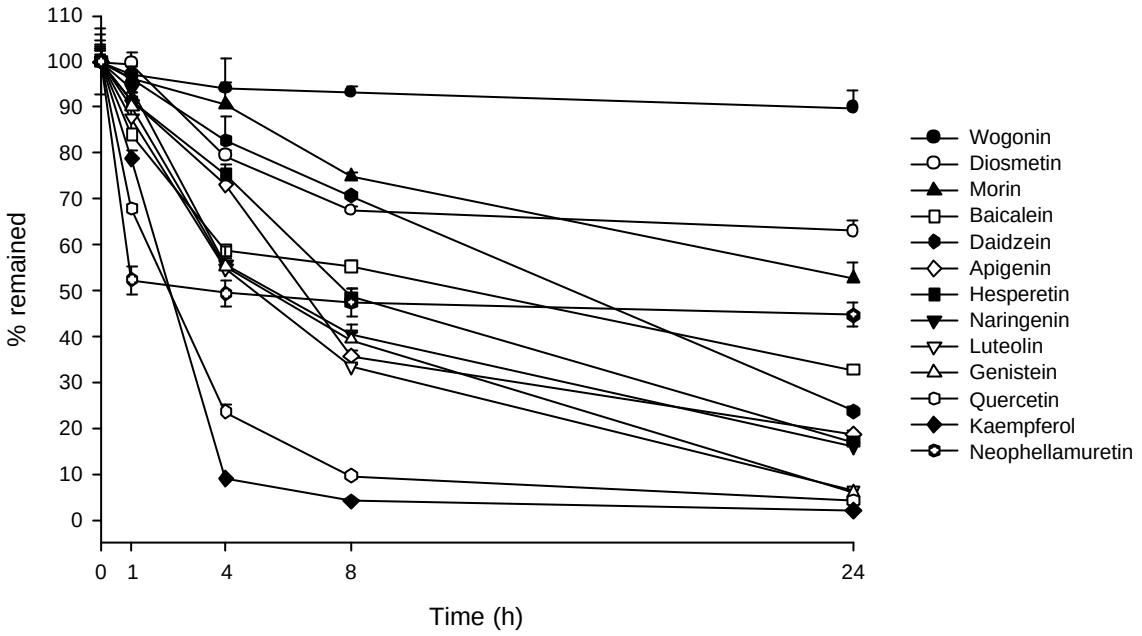

Fig. 9. Degradation of flavonoid aglycones by rat fecal flora (Mean ± S.D. for each time point, n=3).

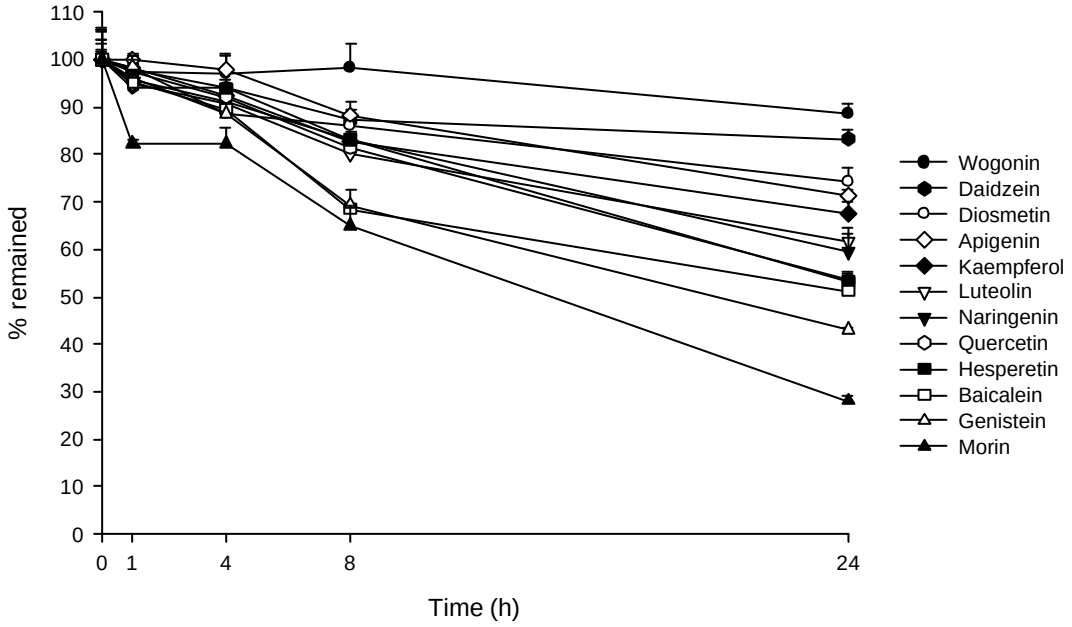

Fig. 10. Degradation of flavonoid aglycones by human fecal flora (Mean ± S.D. for each time point, n=3).

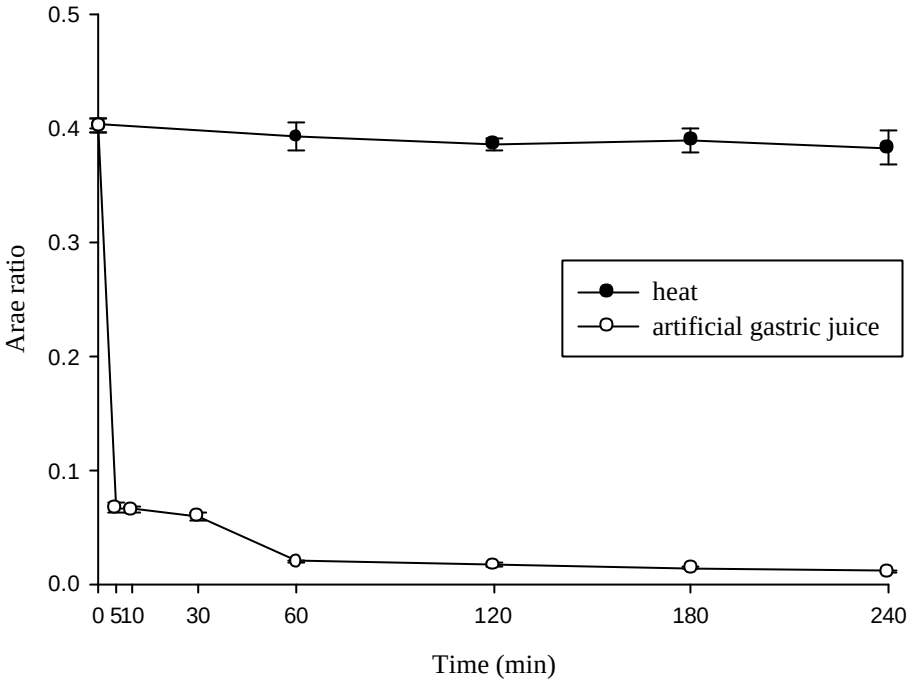

Fig. 11. Mean (± S.D.) peak area ratio-time profiles of catalpol with heating and with artificial gastric juice (n=3).

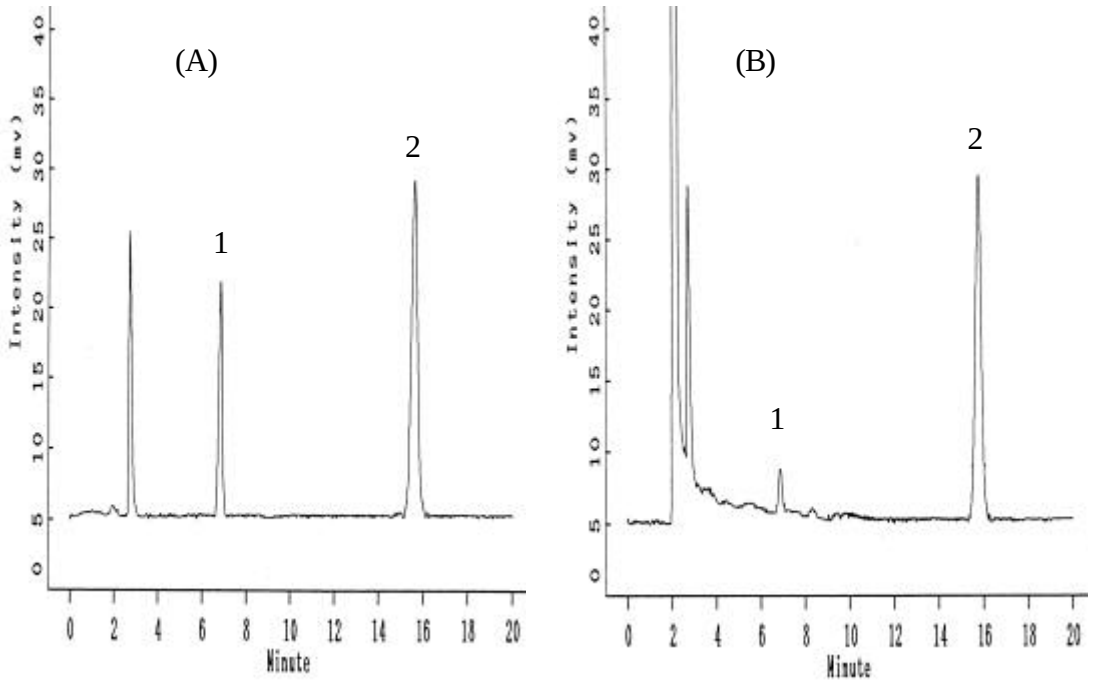

Fig. 12. HPLC chromatograms of catalpol after boiling with water (A) and incubation with artificial gastric juice at 37℃ for 5 min (B). 1: catalpol; 2: 5-hydroxymethyl-2-furaldehyde (HMF, I.S.).

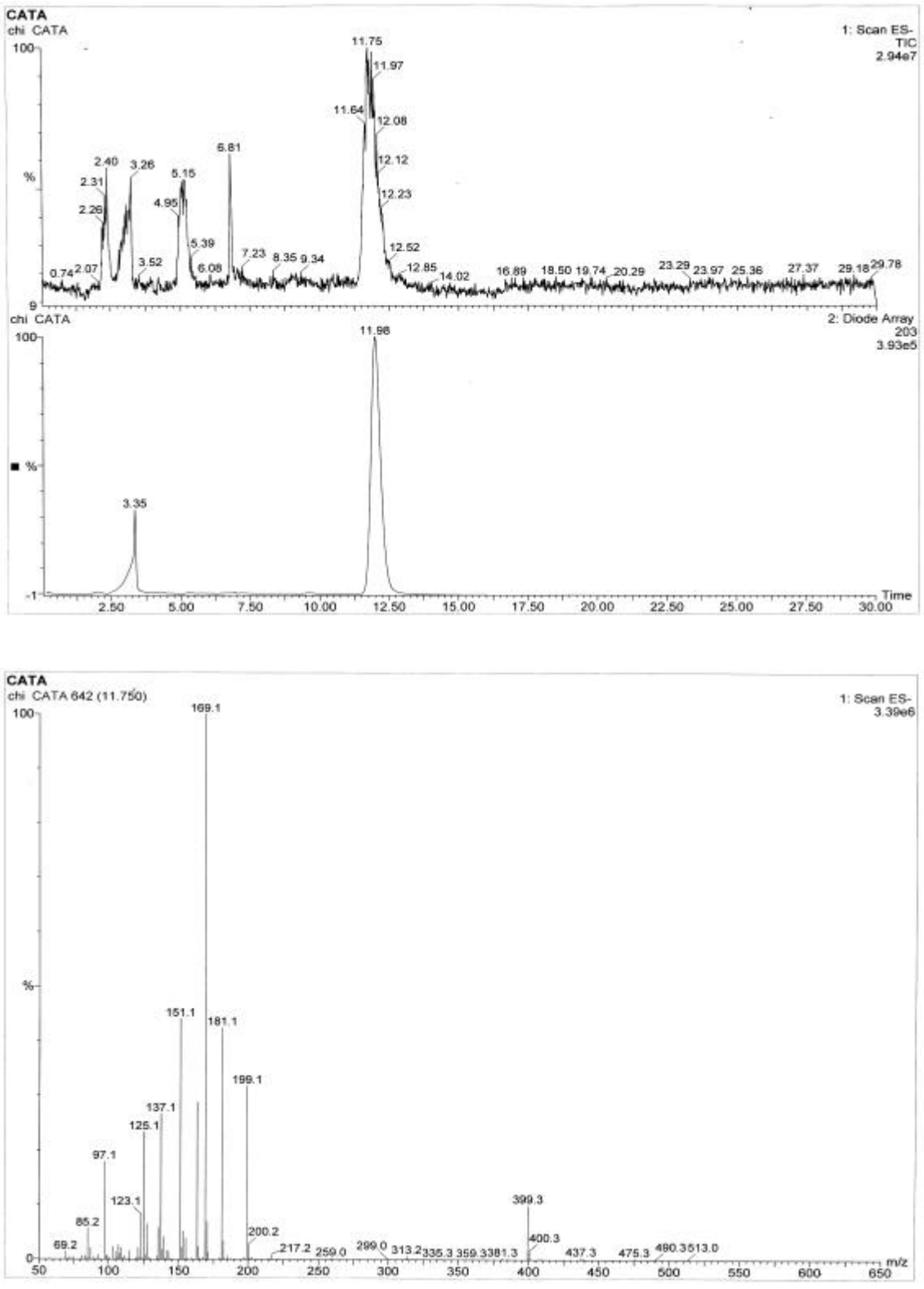

Fig. 13. HPLC/MS chromatograms of catalpol after incubation with β-glucosidase at 37℃ for 2 h.

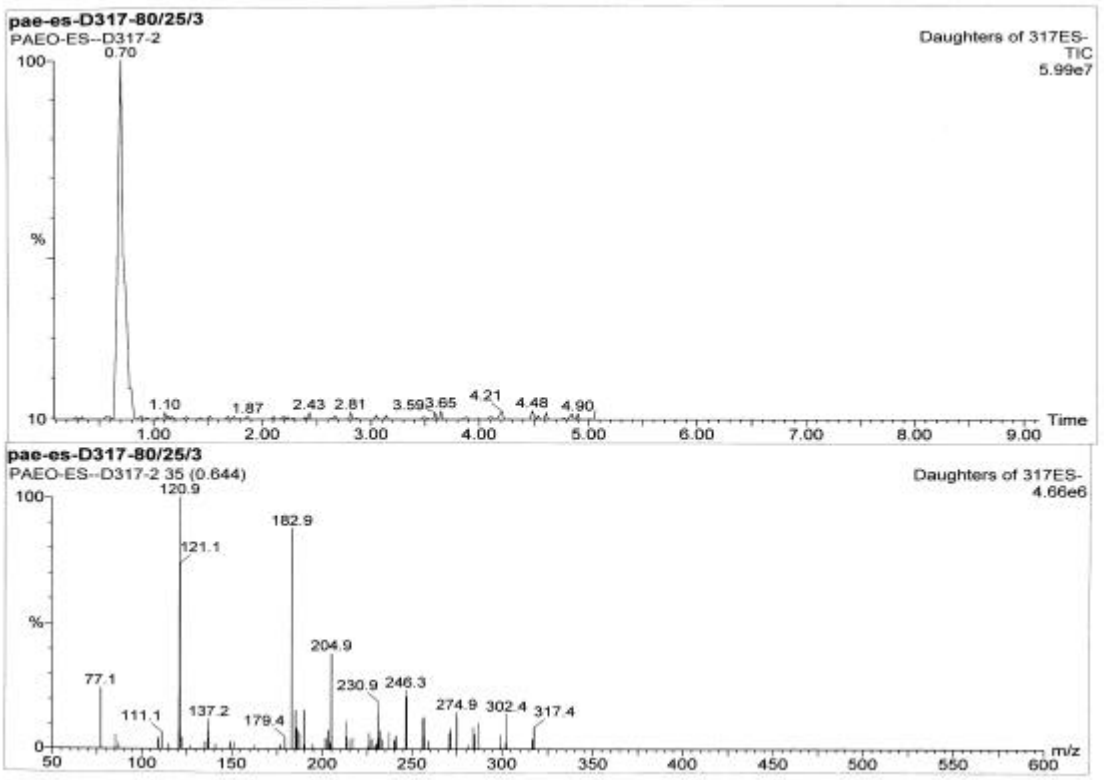

Fig. 14. HPLC/MS chromatogram (upper) and mass spectrum (lower) of paeoniforgenin.

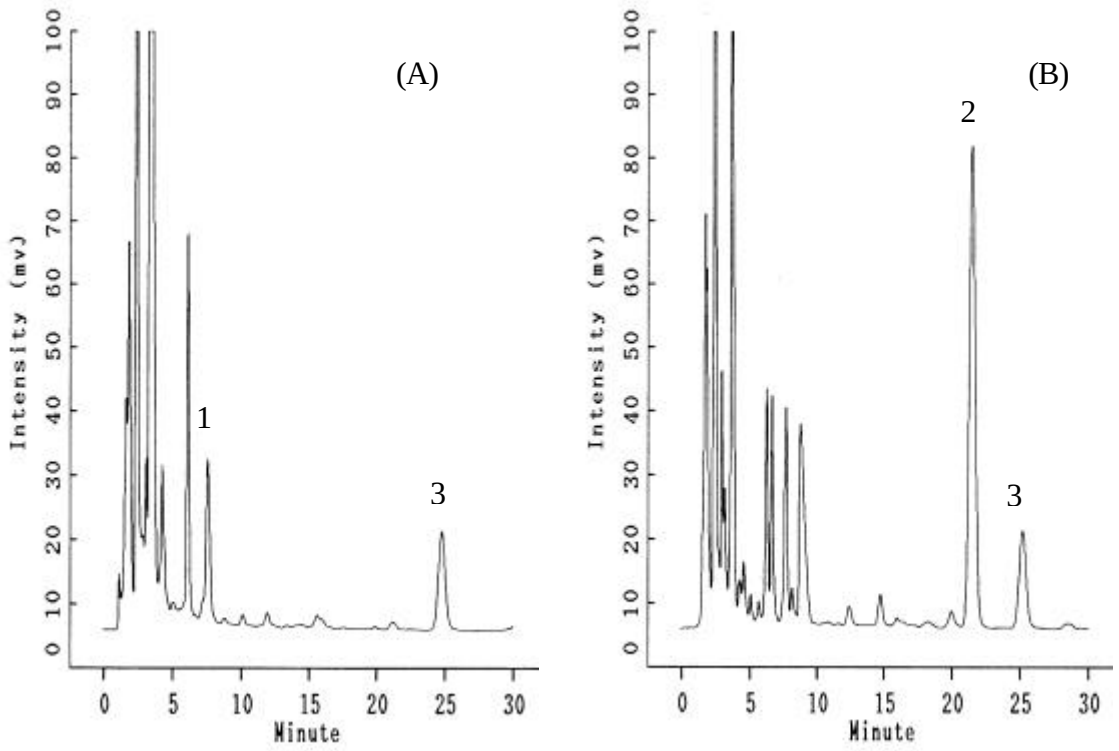

Fig. 15. HPLC chromatograms of traditional decoctions of Paeoniae radix (A) and Paeoniae radix decoction after hydrolysis with 2.4 N HCl (B). 1: paeoniflorin; 2: paeoniforgenin; 3: methylparaben (I.S.).

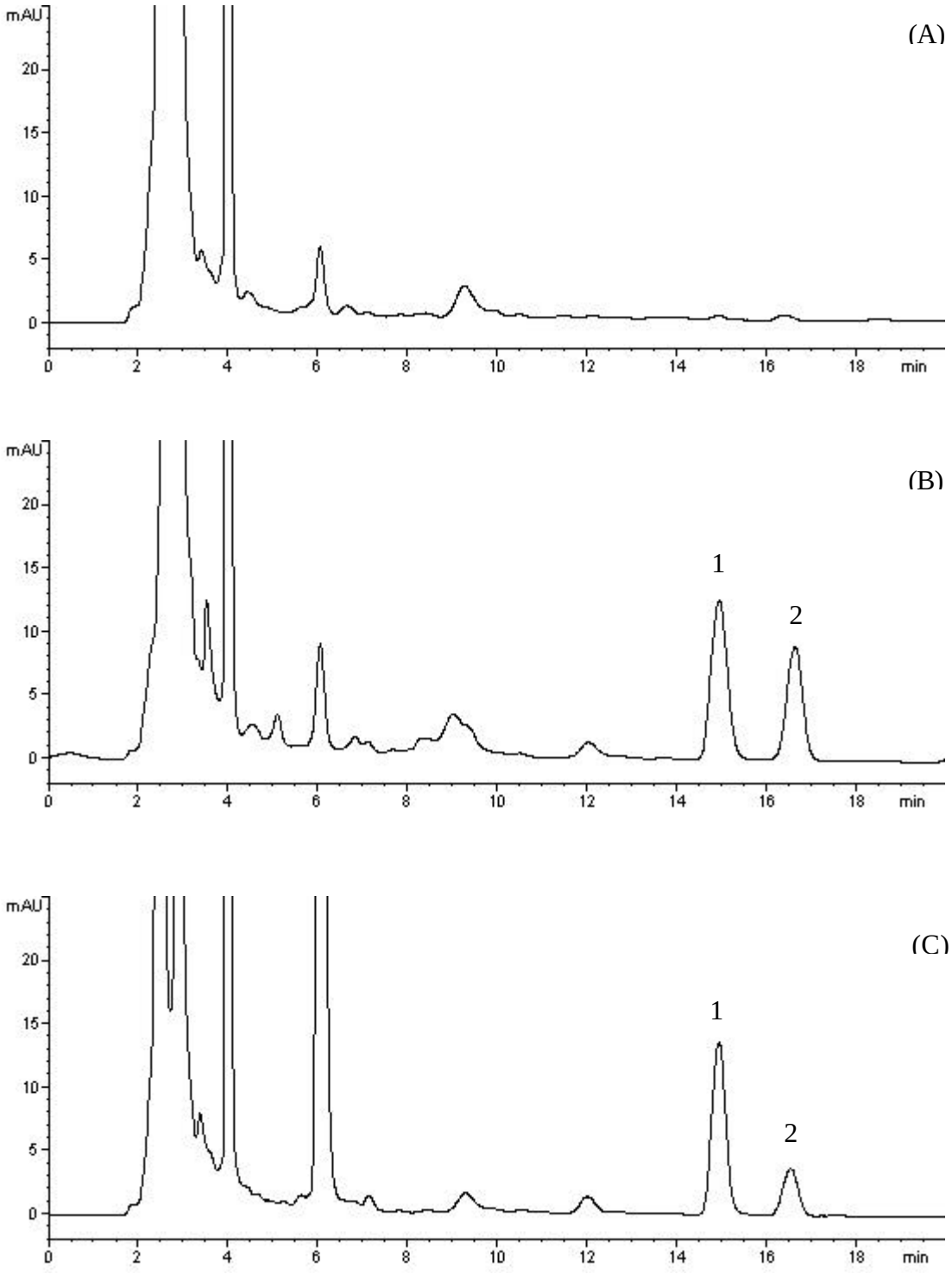

Fig. 16. HPLC chromatograms of paeoniforgenin with internal standard in rat serum: blank serum (A); blank serum spiked with paeoniforgenin and internal standard (B); serum sample obtained 10 min after oral administration of Paeoniae radix decoction (C). 1: paeoniforgenin; 2: methylparaben (I.S.).

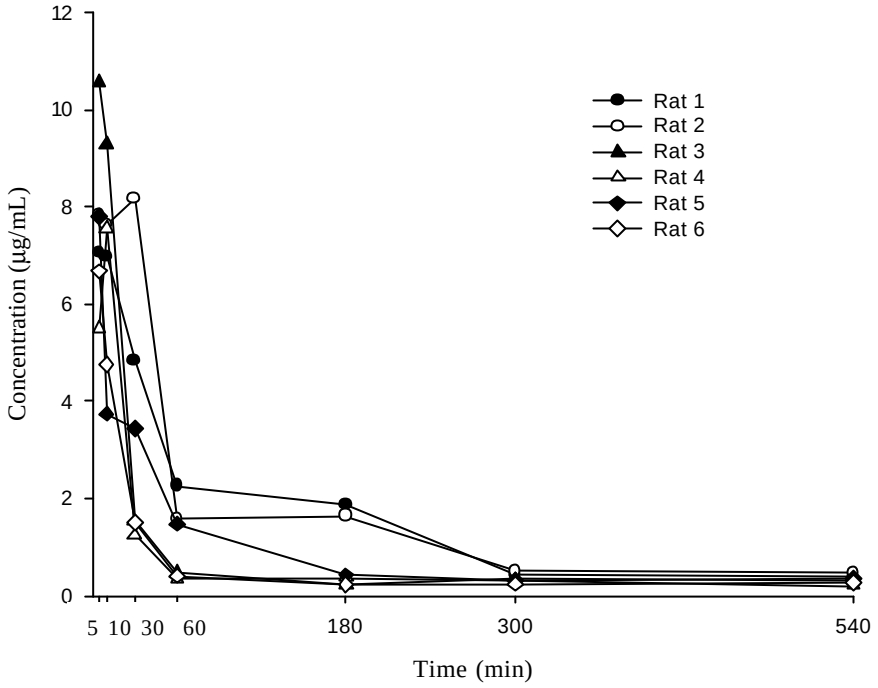

Fig. 17. Serum concentration-time profiles of paeoniforgenin after oral administration of Paeoniae radix decoction to six rats.

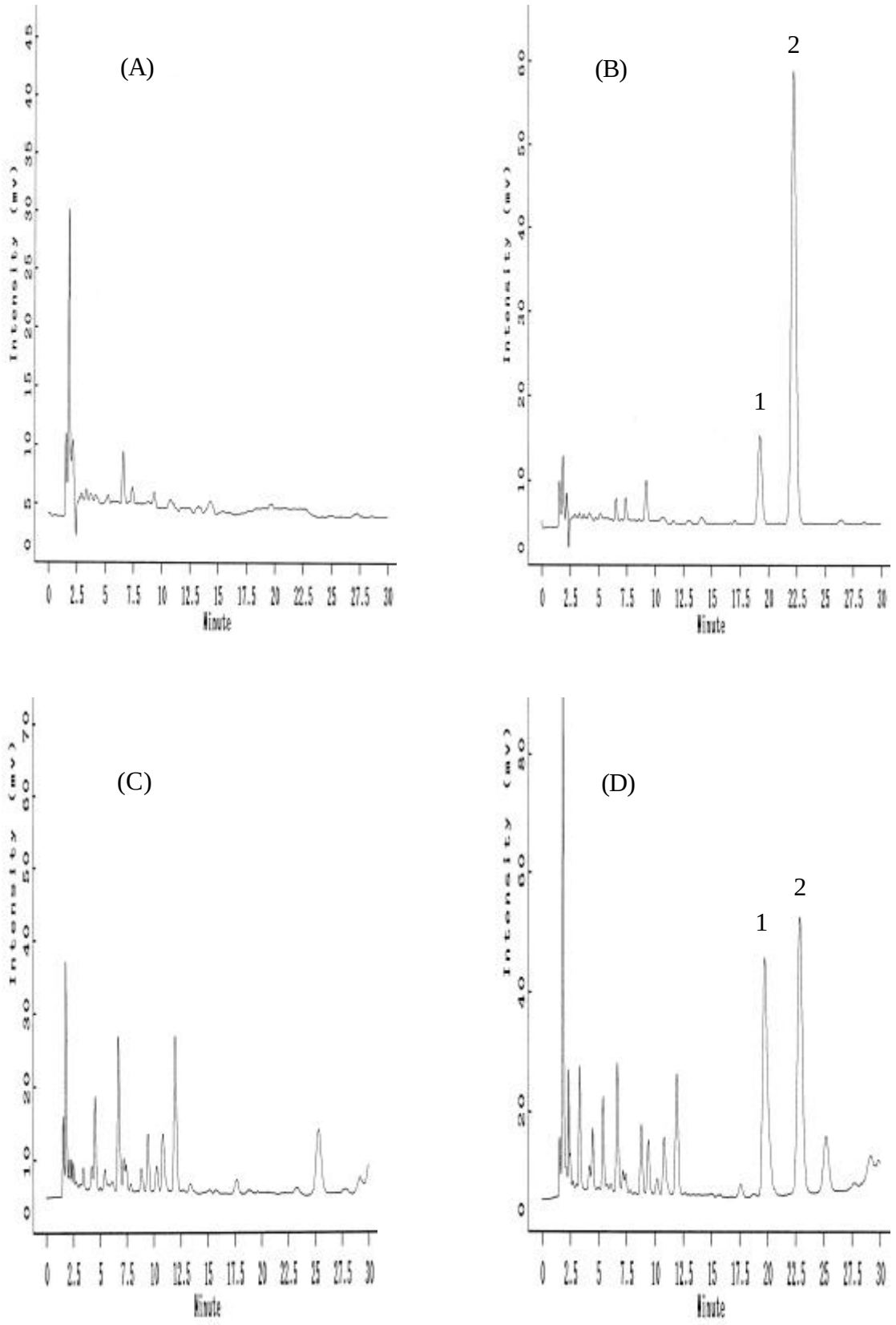

Fig. 18. HPLC chromatograms of rabbit (A) and rat (C) blank feces; paeoniforgenin after incubation of paeoniflorin with rabbit (B) and rat (D) feces. 1: paeoniforgenin; 2: methylparaben (IS).

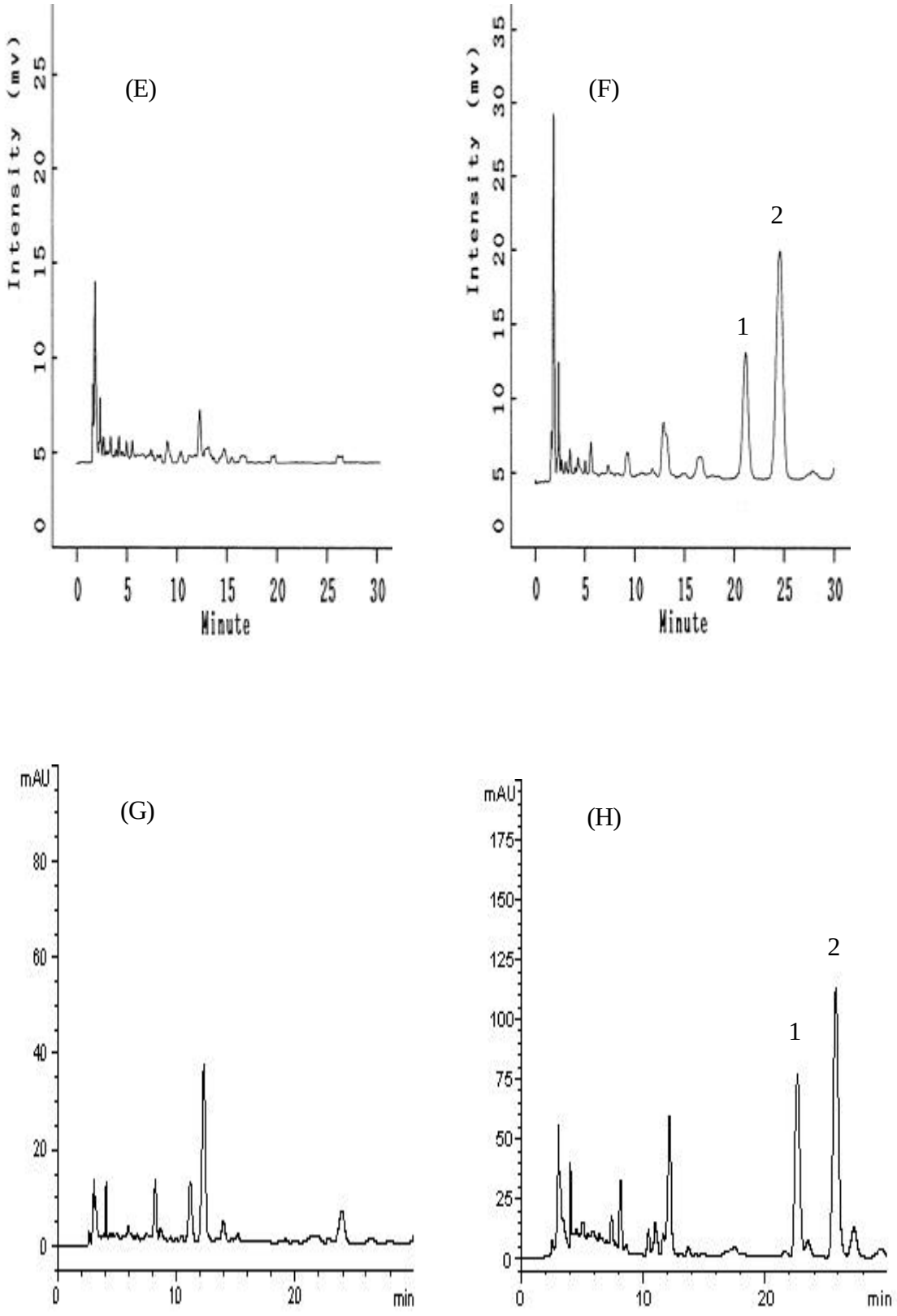

Fig. 19. HPLC chromatograms of human (E) and pig (G) blank feces; paeoniforgenin after incubation of paeoniflorin with human (F) and pig (H) feces. 1: paeoniforgenin; 2: methylparaben (IS).

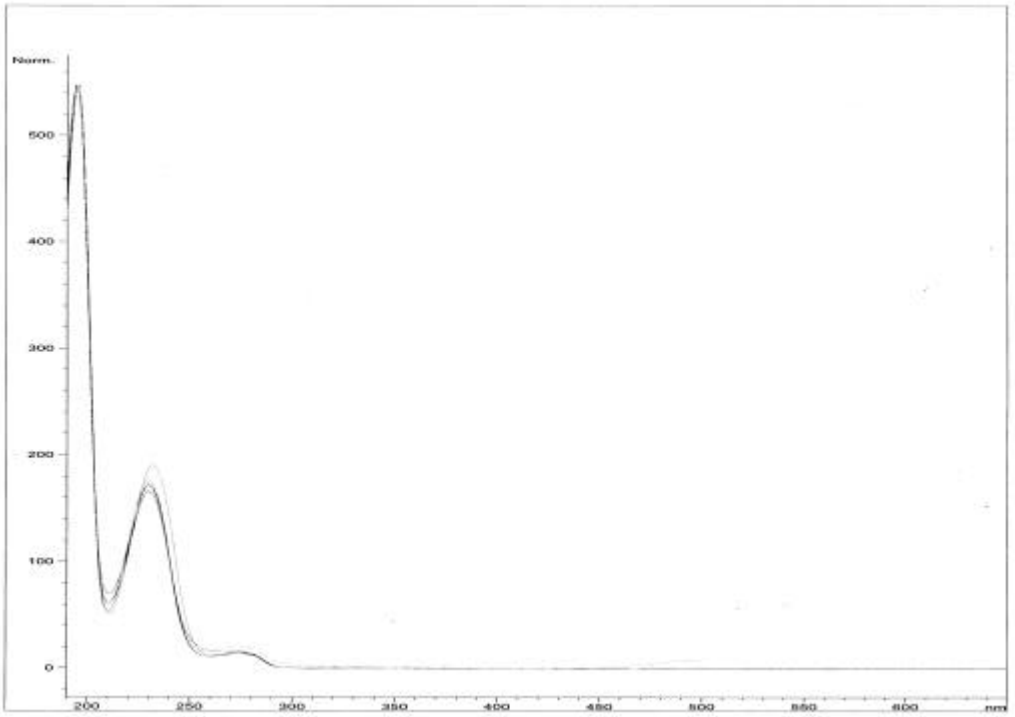

Fig. 20. UV spectrums of paeoniforgenin after incubation of paeoniflorin with rat, rabbit, pig and human feces.

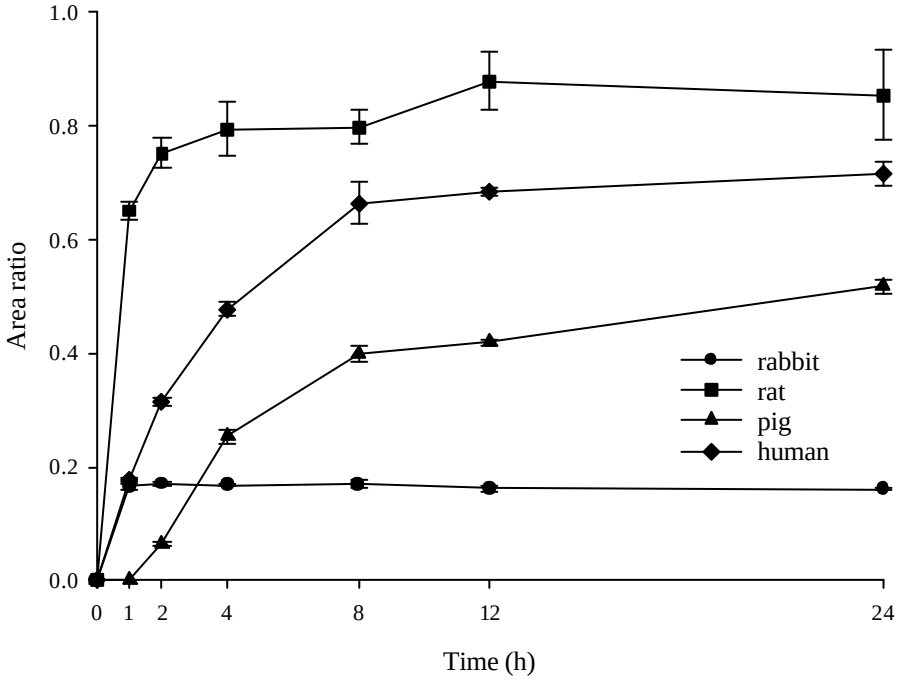

Fig. 21. Mean (± S.D.) peak area ratio-time profiles of paeoniforgenin after incubation of paeoniflorin with rabbit, rat, pig and human feces (n=3).

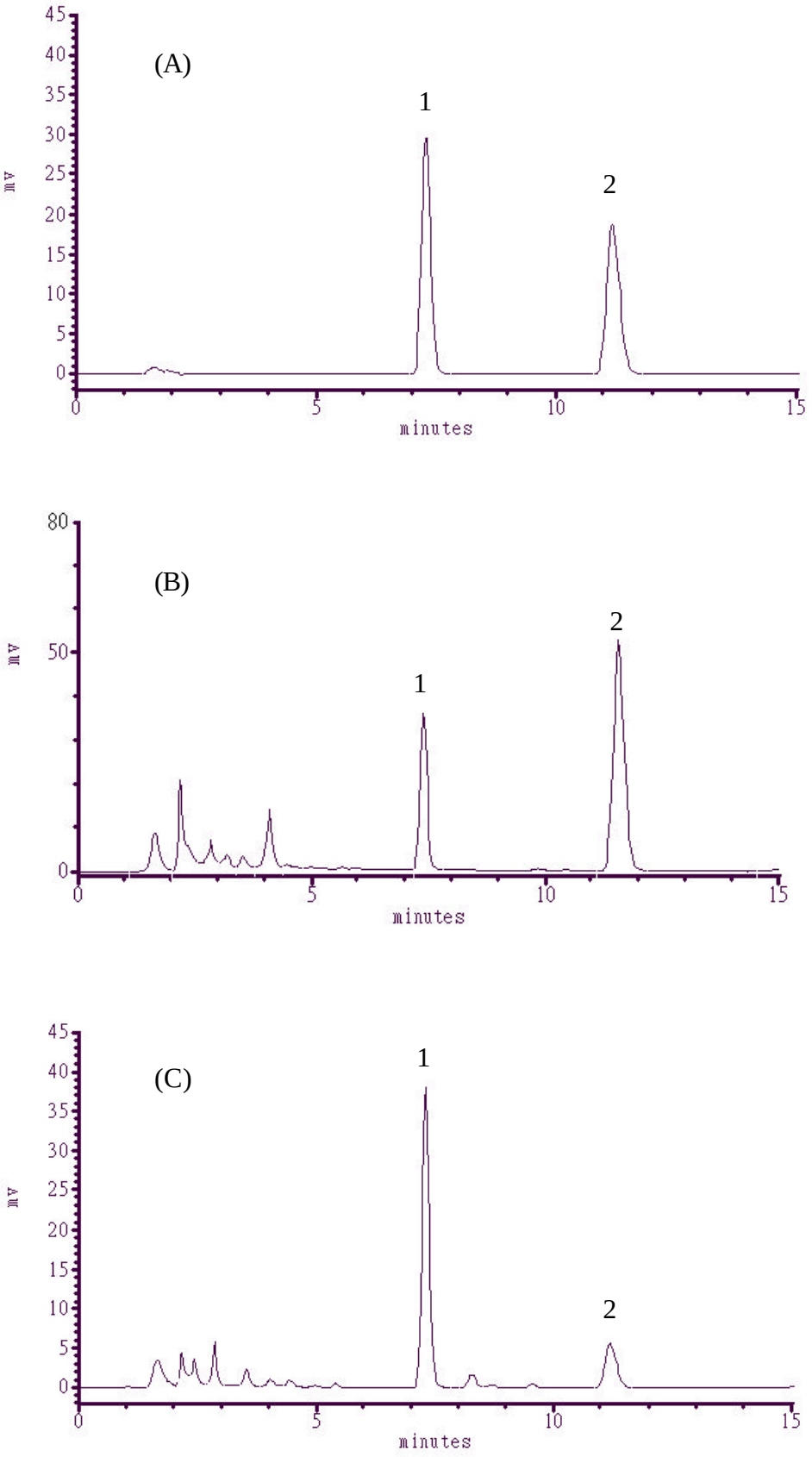

Fig. 22. HPLC chromatograms of 6,7-dimethoxycoumarin (I.S.; 1) and quercetin (2) in methanol solution (A); after hydrolysis of onion juice (B) and Huaimi infusion (C).

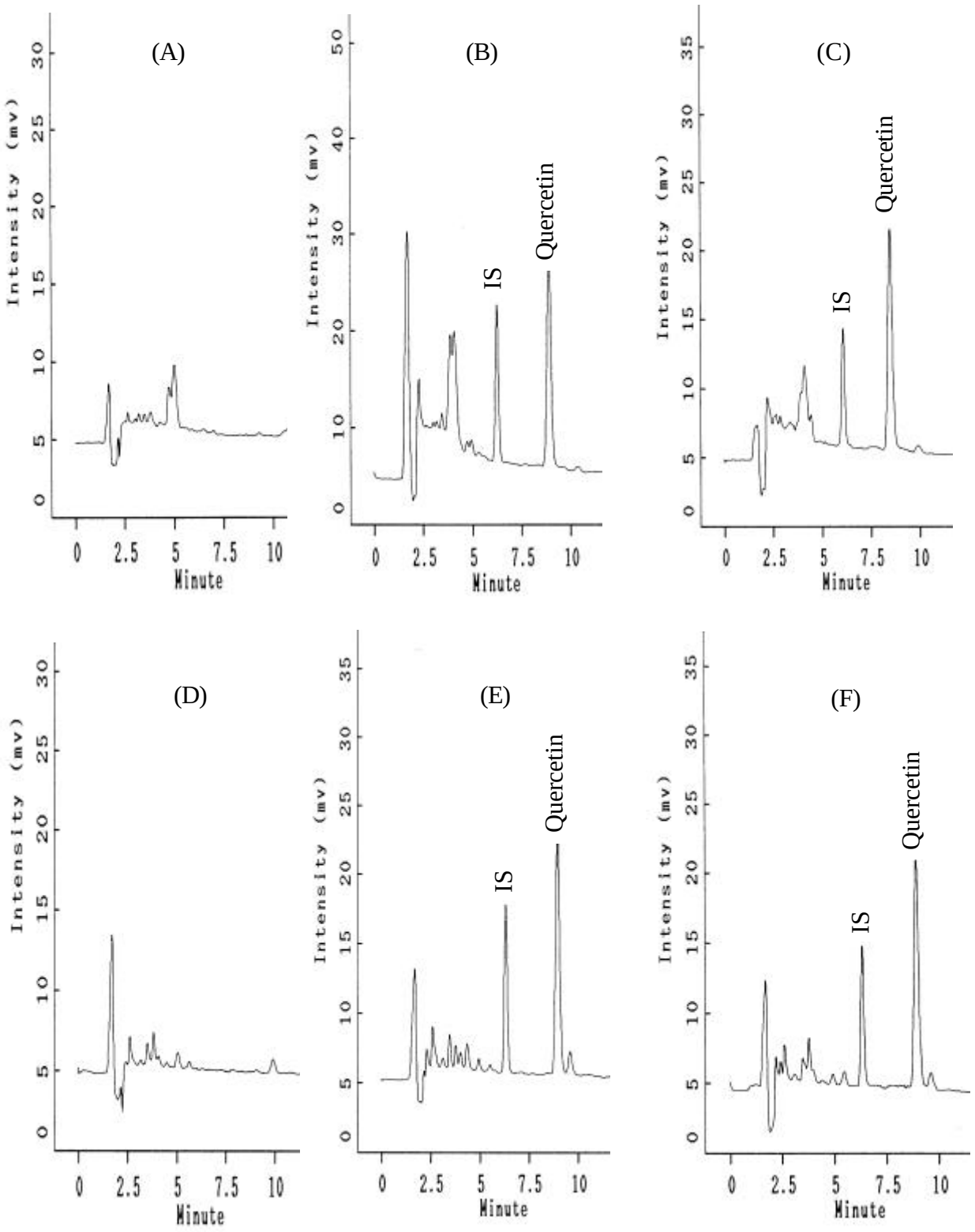

Fig. 23. HPLC chromatograms of human blank feces (A); quercetin obtained after incubation of onion juice (B) and Huaimi infusion (C) with human feces; rat blank feces (D); quercetin obtained after incubation of onion juice (E) and Huaimi infusion (F) with rat feces. IS: 6,7-dimethoxycoumarin.

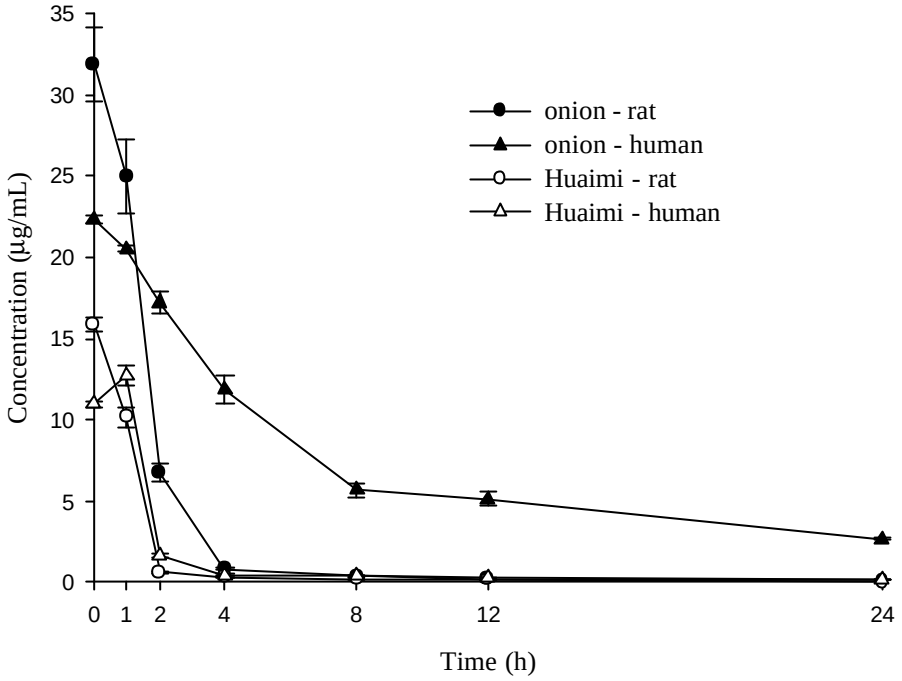

Fig. 24. Mean (± S.D.) concentration-time profiles of quercetin after incubation of onion and Huaimi infusion in rat and human feces (n=3).

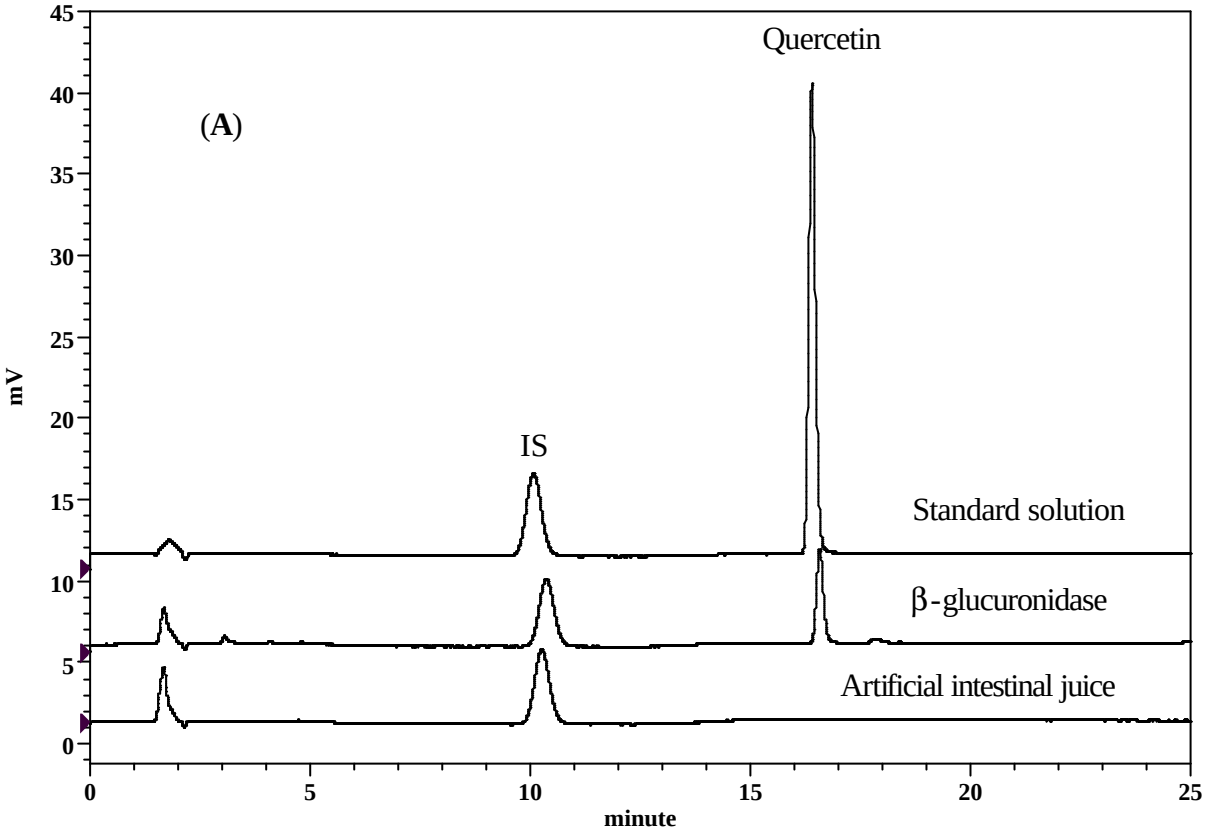
(A)
Quercetin
IS
Standard solution
β-glucuronidase
Artificial intestinal juice
mV
minute
0
5
10
15
20
25
30
35
40
45

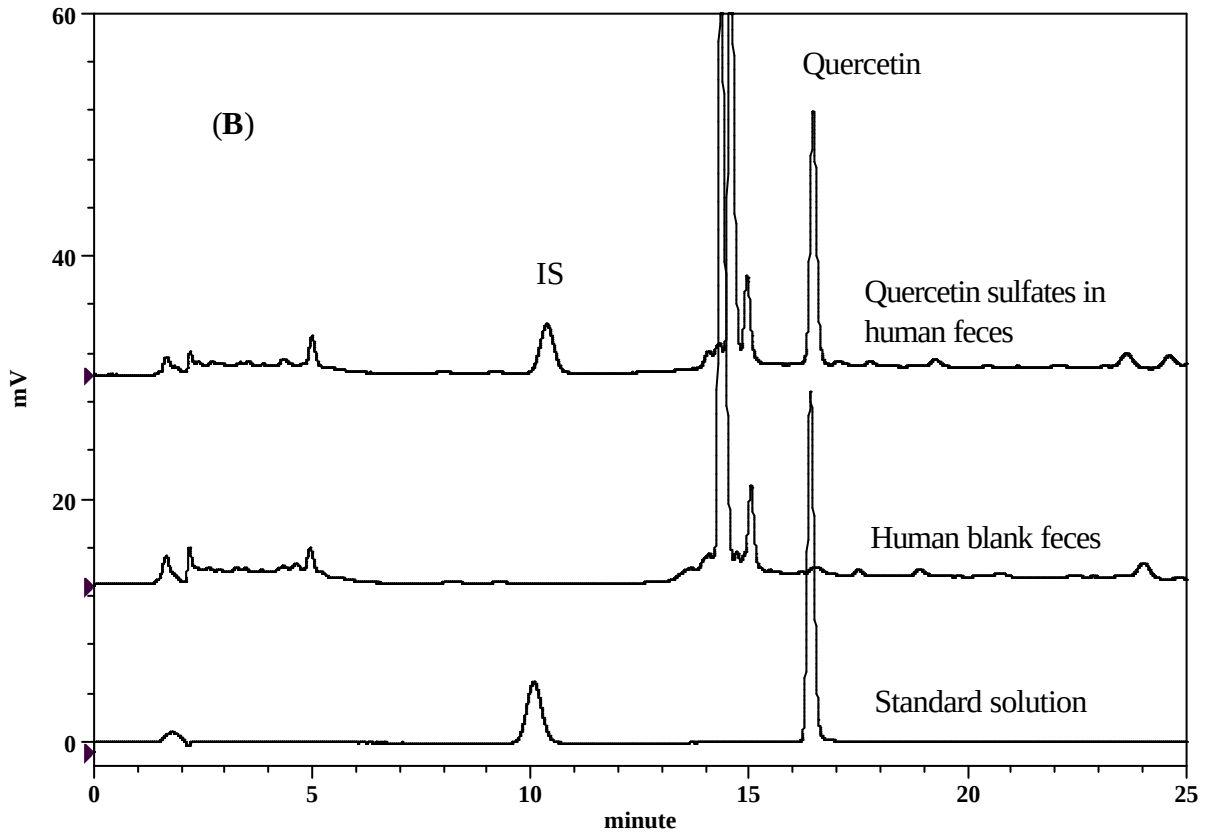
(B)
Quercetin
IS
Quercetin sulfates in human feces
Human blank feces
Standard solution
mV
minute
0
20
40
60
0
5
10
15
20
25

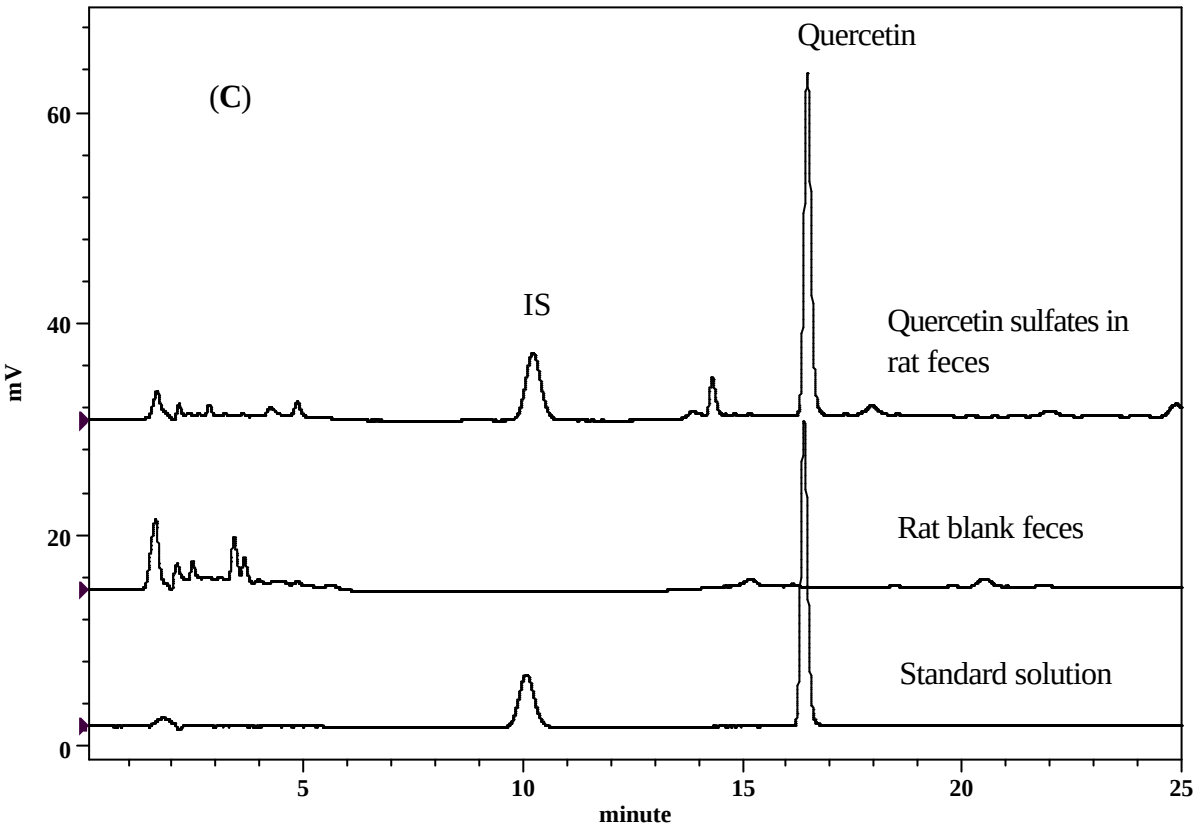

Fig. 25. HPLC chromatograms of quercetin in standard solution and after incubation of quercetin sulfates with β-glucuronidase and with artificial intestinal juice (A); with human feces and human blank feces (B); with rat feces and rat blank feces (C); with 6,7-dimethoxycoumarin as the internal standard (IS).

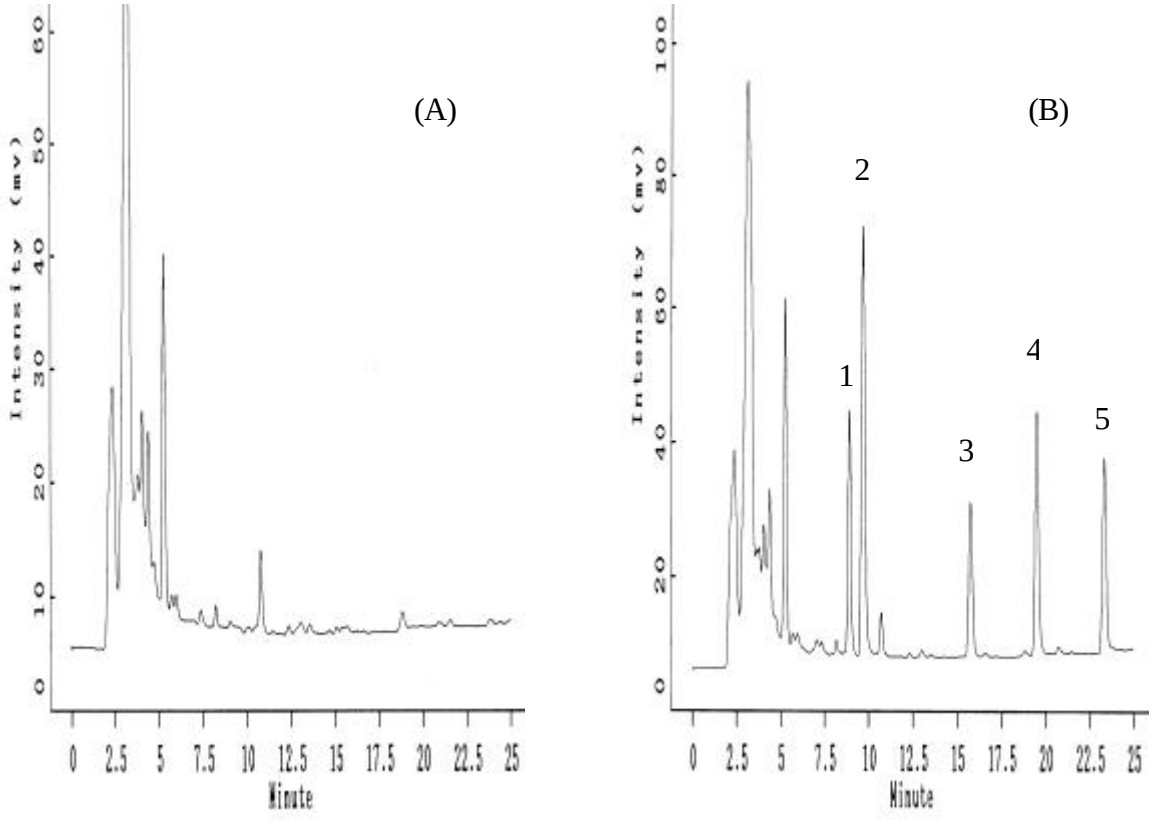

Fig. 26. HPLC chromatograms of blank feces (A); and anthraquinones obtained after incubation of rubarb decoction with rat feces (B) 1: aloe-emodin; 2: rhein; 3: emodin; 4: 2-methylanthraquinone (I.S.); 5: chrysophanol.

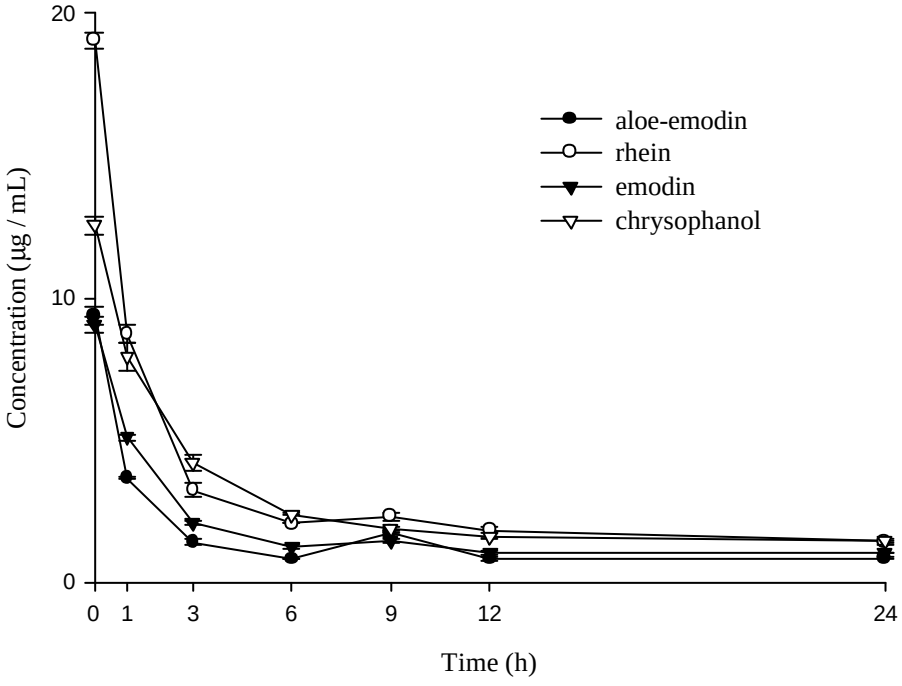

Fig. 27. Mean (± S.D.) concentration-time profiles of aloe-emodin, rhein, emodin and chrysophanol after incubation of rubarb decoction with rat feces (n=3).

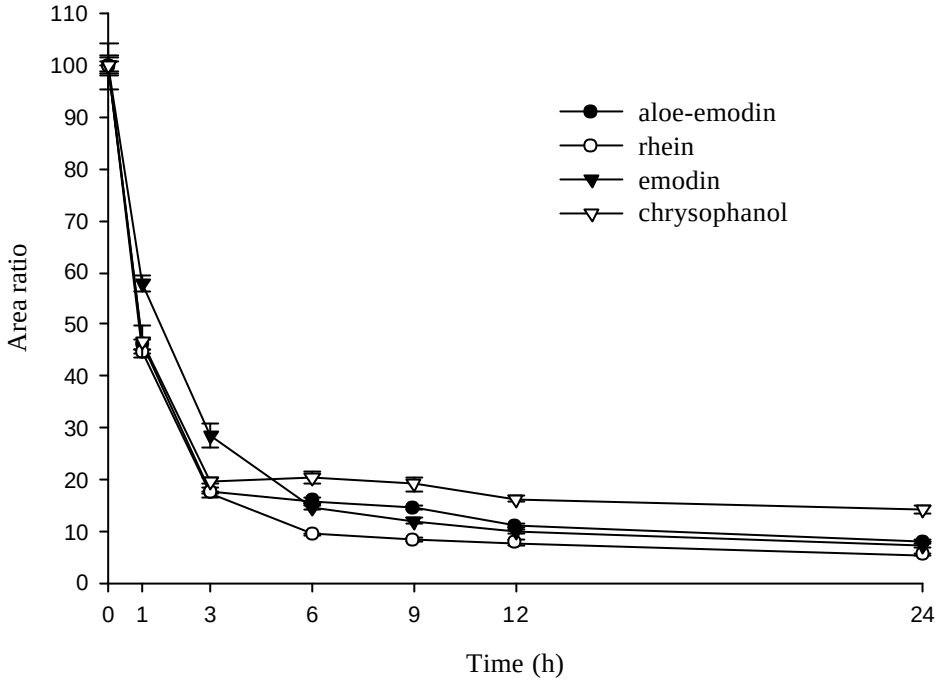

Fig. 28. Mean (± S.D.) peak area ratio-time profiles of aloe-emodin, rhein, emodin and chrysophanol after incubation with rat feces (n=3), respectively.

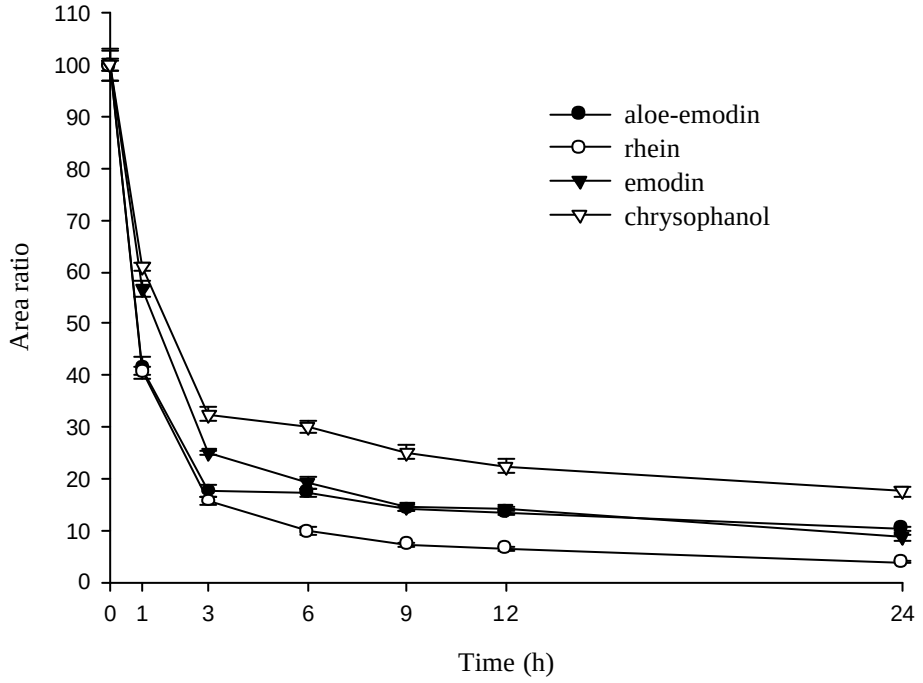

Fig. 29. Mean (± S.D.) peak area ratio-time profiles of aloe-emodin, rhein, emodin and chrysophanol after incubation of their mixture with rat feces (n=3).

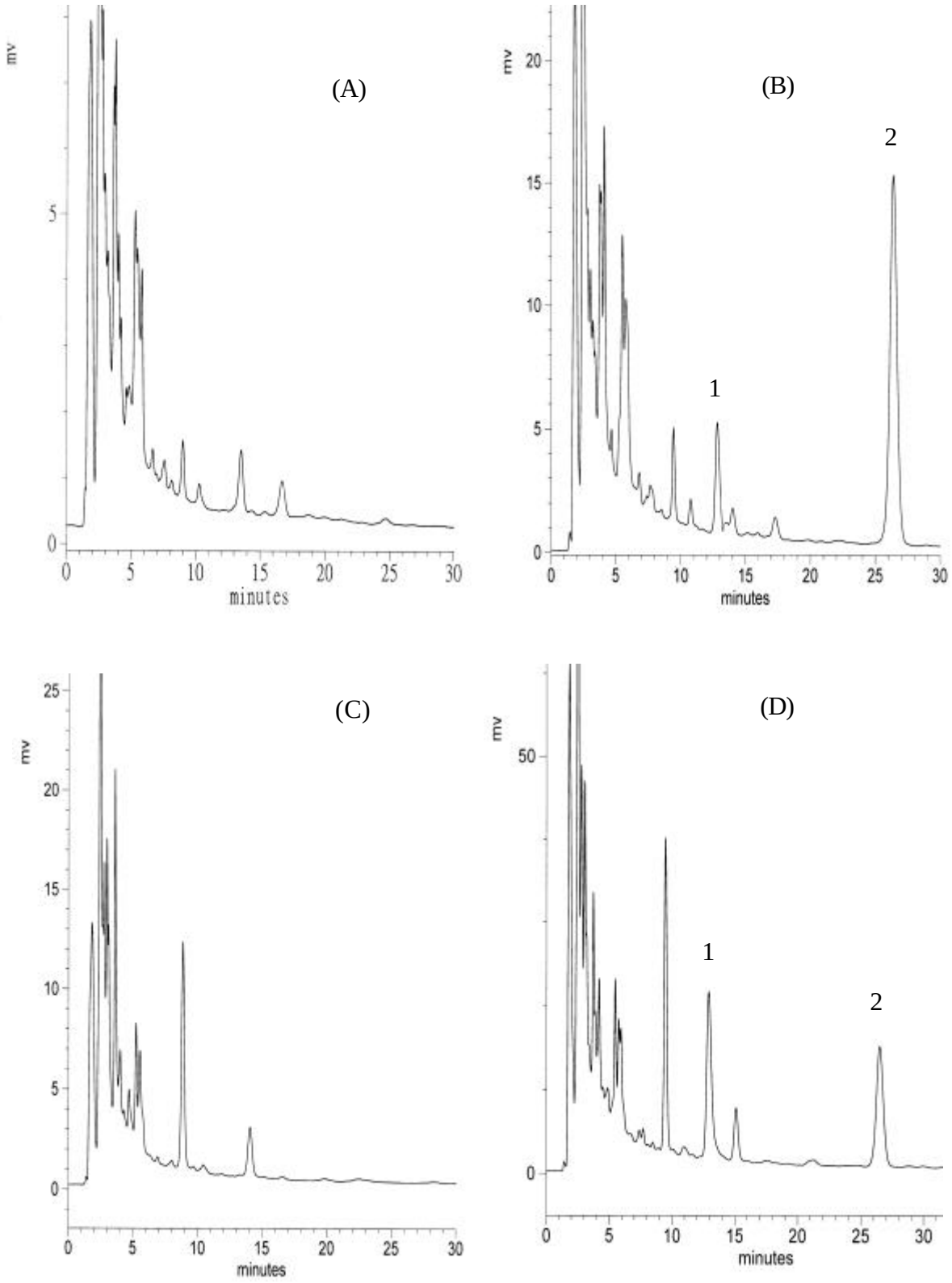

Fig. 30. HPLC chromatograms of rabbit blank feces (A); sennoside A incubated with rabbit feces (B); rat blank feces (C) and sennoside B incubated with rat feces (D) 1: rhein; 2: amylparaben (I.S.).

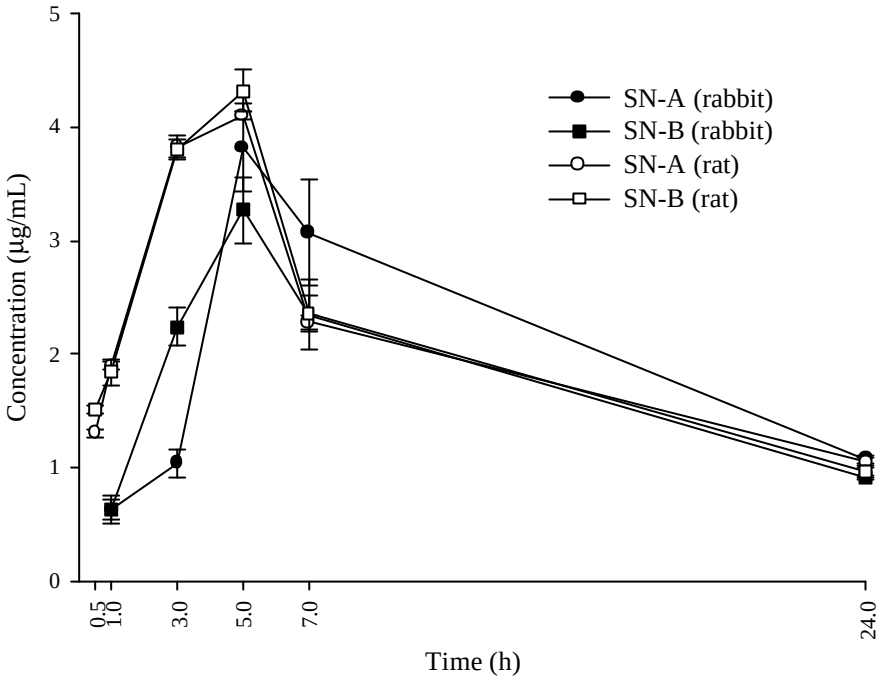

Fig. 31. Mean (± S.D.) concentration-time profiles of rhein after incubation of sennosides A and B with rabbit and rat feces (n=3), respectively.

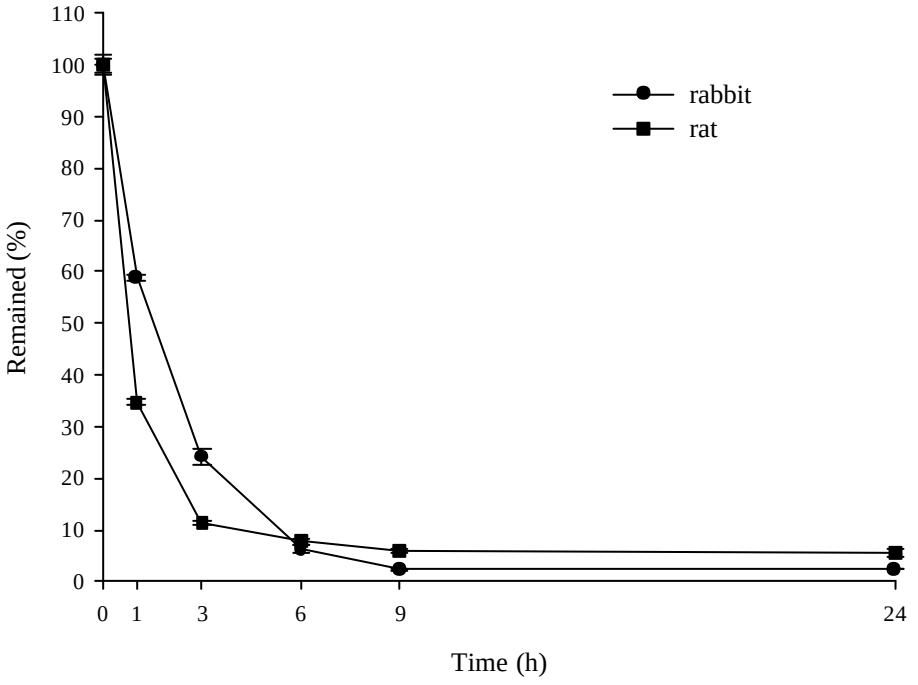

Fig. 32. Degradation of rhein by rabbit and rat feces (Mean ± S.D. for each time point, n=3).

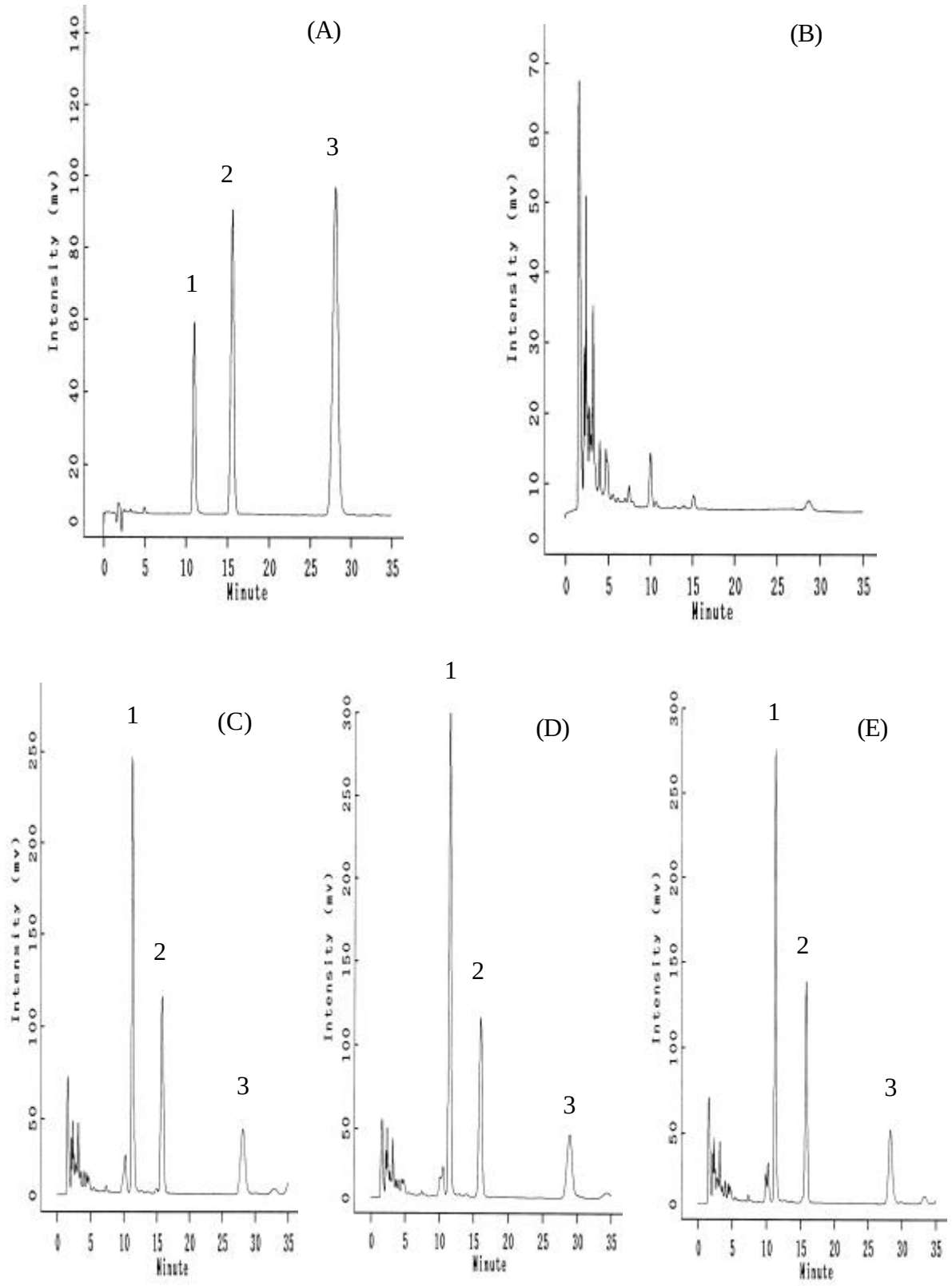

Fig. 33. HPLC chromatograms of standard solution (A); blank feces (B); baicalein and wogonin obtained after incubation of S (C), SFW (D) or HTS (E) with rat feces. 1: baicalein; 2: propylparaben (I.S.); 3: wogonin.

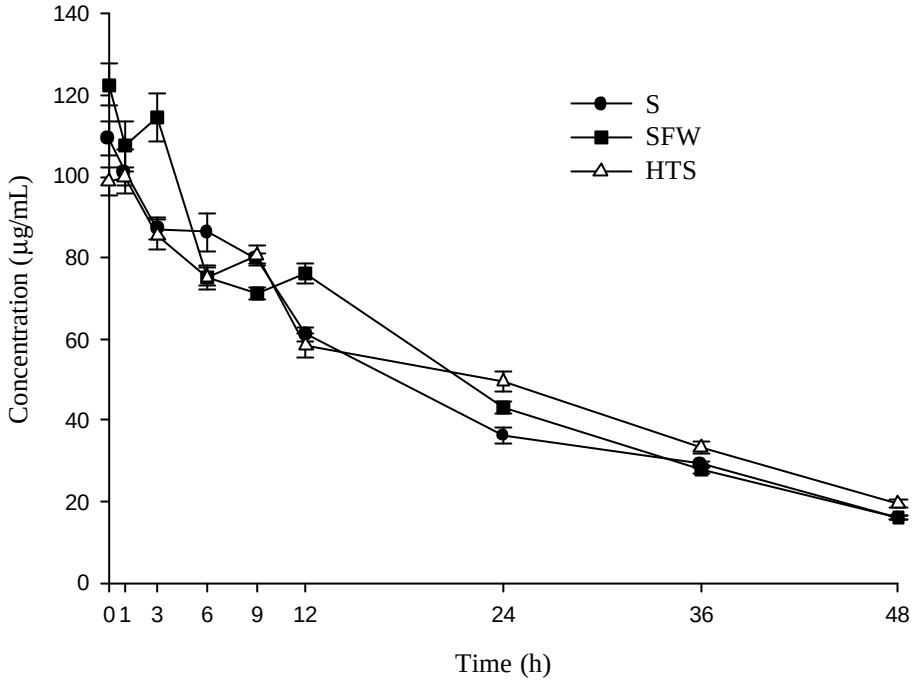

Fig. 34. Mean (± S.D.) concentration-time profiles of baicalein after incubation of S, SFW or HTS with rat feces (n=3). S: Scutellariae Radix, SFW: Scutellariae Radix fried with wine, HTS: honey-treated Scutellariae Radix.

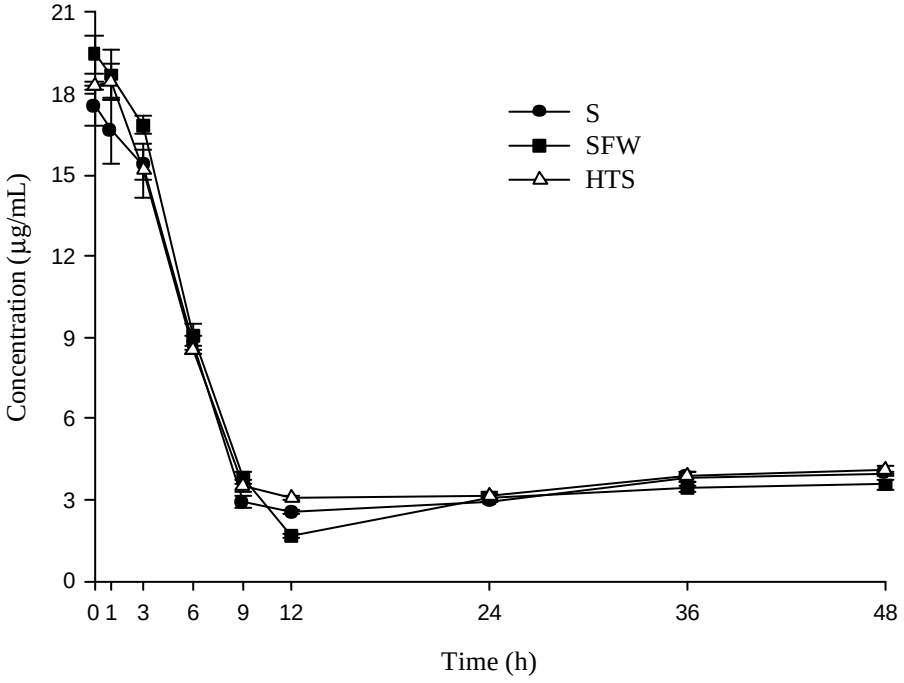

Fig. 35. Mean (± S.D.) concentration-time profiles of wogonin after incubation of S, SFW or HTS with rat feces (n=3). S: Scutellariae Radix, SFW: Scutellariae Radix fried with wine, HTS: honey-treated Scutellariae Radix.

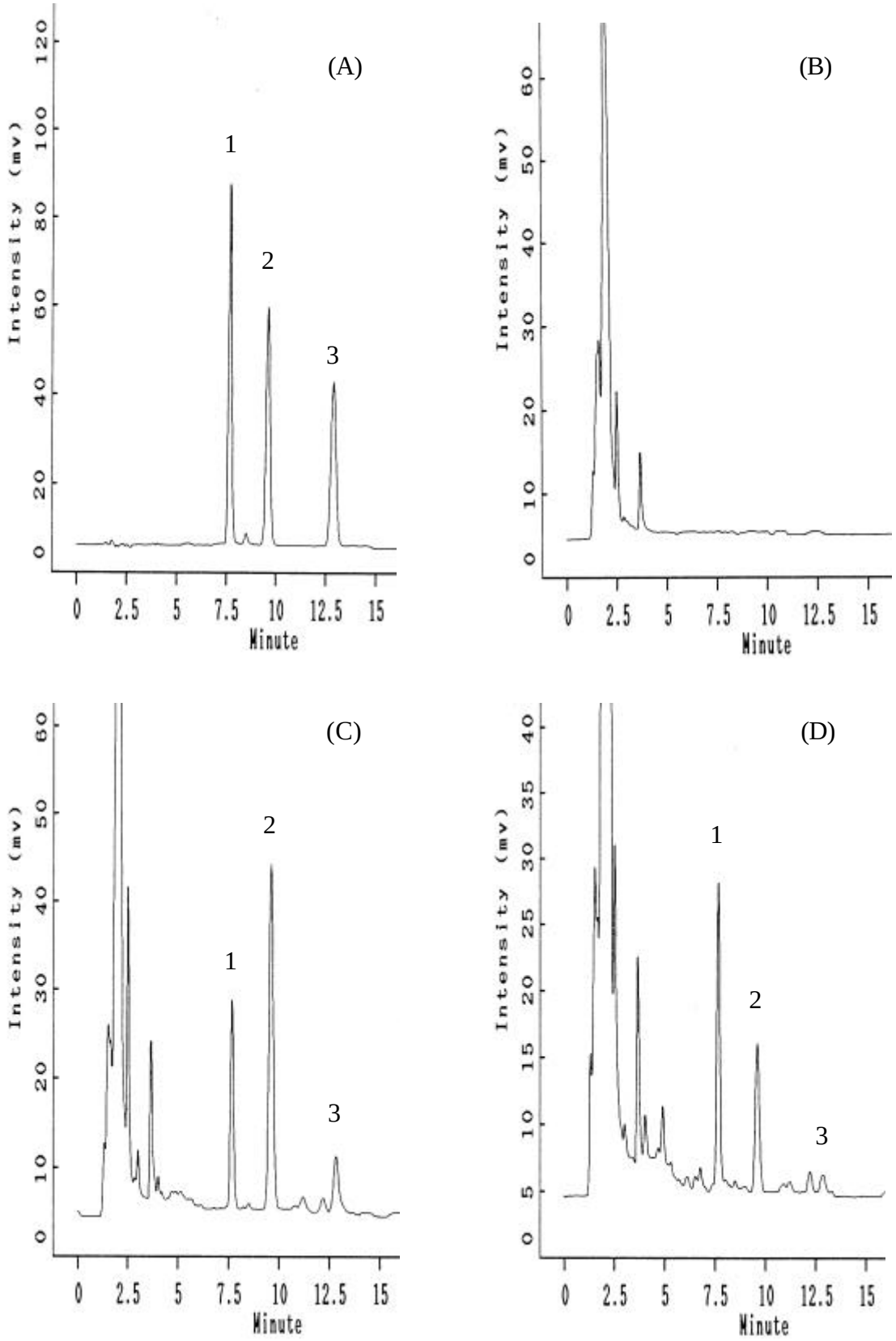

Fig. 36. HPLC chromatograms of standard solution (A); blank feces (B); GA and 3-dehydroGA obtained after incubation of glycyrrhizin (C) and licorice decoction (D) with pig feces. 1: 2-methylanthraquinone (I.S.); 2: glycyrrhetic acid (GA); 3: 3-dehydroGA.

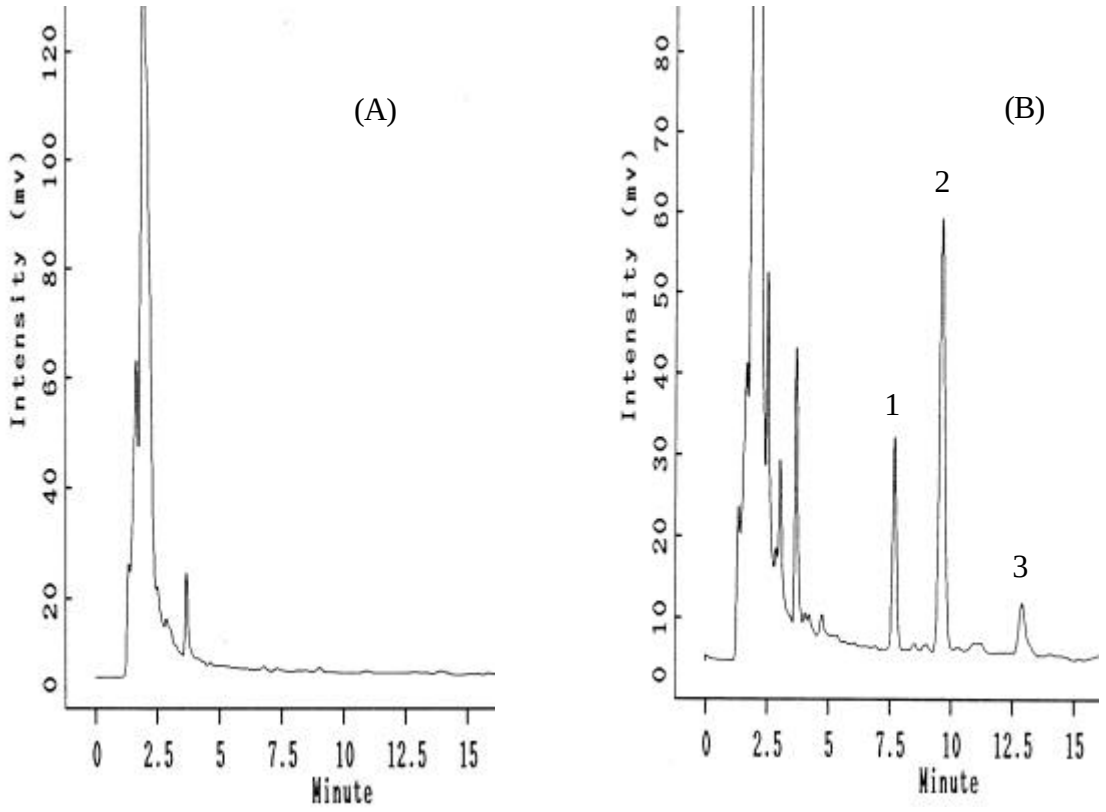

Fig. 37. HPLC chromatograms of blank feces (A); GA and 3-dehydroGA obtained after incubation of glycyrrhizin (B) and licorice decoction (C) with rat feces.

1: 2-methylanthraquinone (I.S.)

2: GA

3: 3-dehydroGA

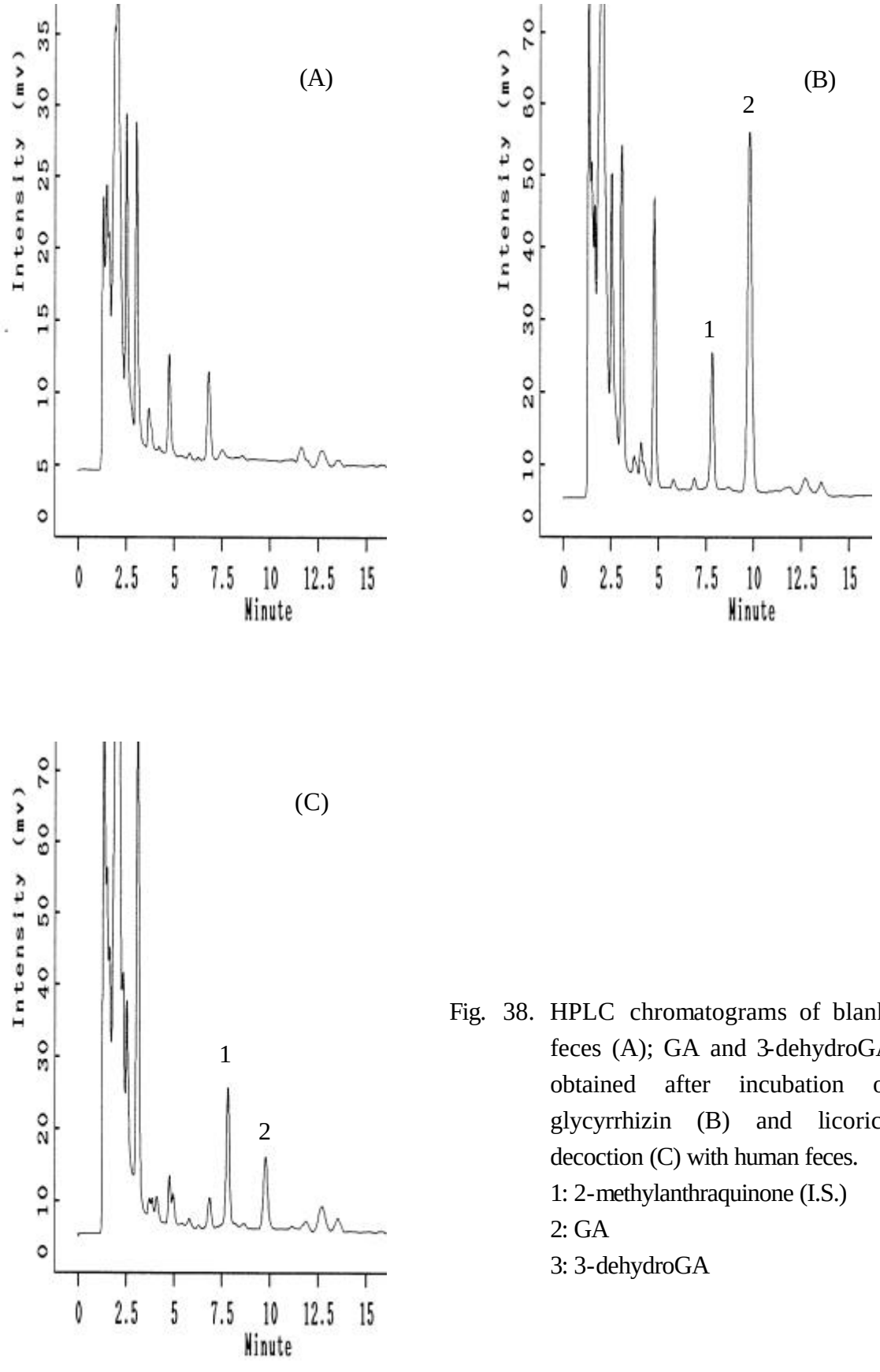

Fig. 38. HPLC chromatograms of blank feces (A); GA and 3-dehydroGA obtained after incubation of glycyrrhizin (B) and licorice decoction (C) with human feces.
1: 2-methylanthraquinone (I.S.)
2: GA
3: 3-dehydroGA

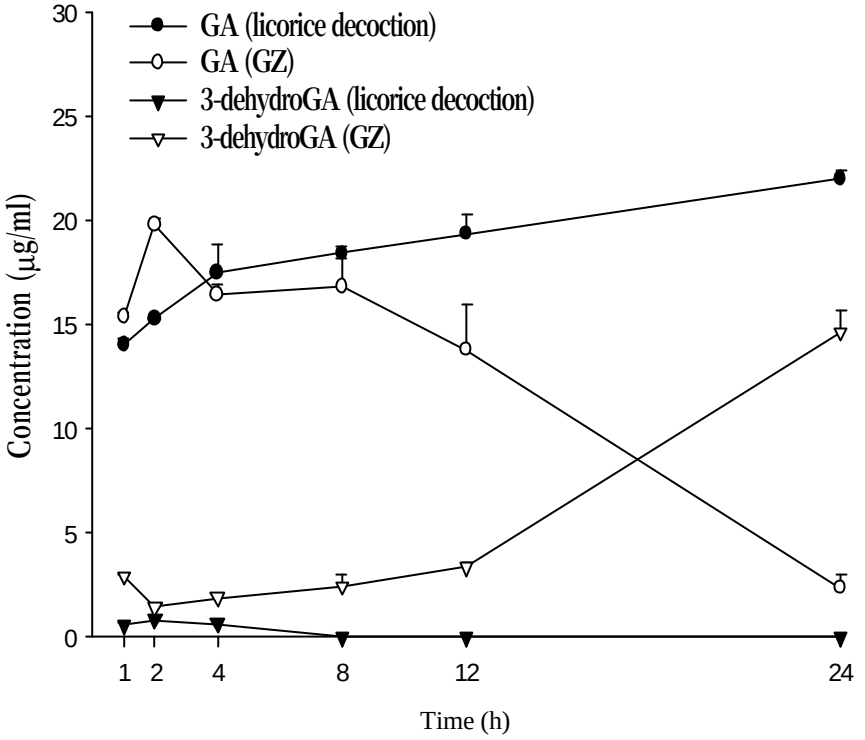

Fig. 39. Mean (± S.D.) concentration-time profiles of GA and 3-dehydroGA after incubation of glycyrrhizin or licorice decoction with rabbit feces (n=3).

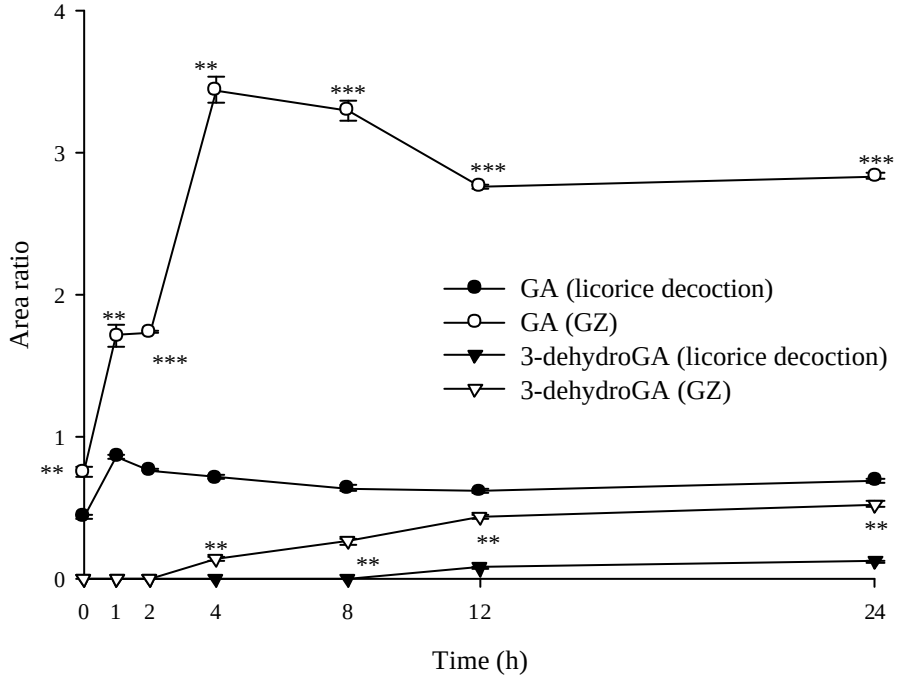

Fig. 40. Mean (± S.D.) peak area ratio-time profiles of GA and 3-dehydroGA after incubation of glycyrrhizin or licorice decoction with rat feces (n=3).

* $p<0.05$, ** $p<0.01$, *** $p<0.001$ compared with licorice decoction.

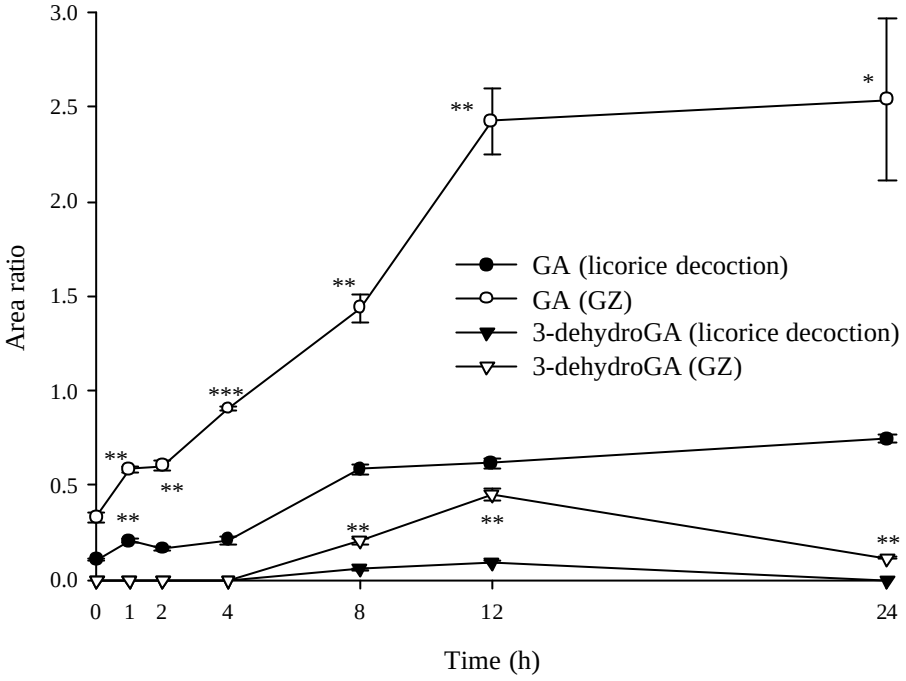

Fig. 41. Mean (± S.D.) peak area ratio-time profiles of GA and 3-dehydroGA after incubation of glycyrrhizin or licorice decoction with pig feces (n=3).

* $p < 0.05$, ** $p < 0.01$, *** $p < 0.001$ compared with licorice decoction.

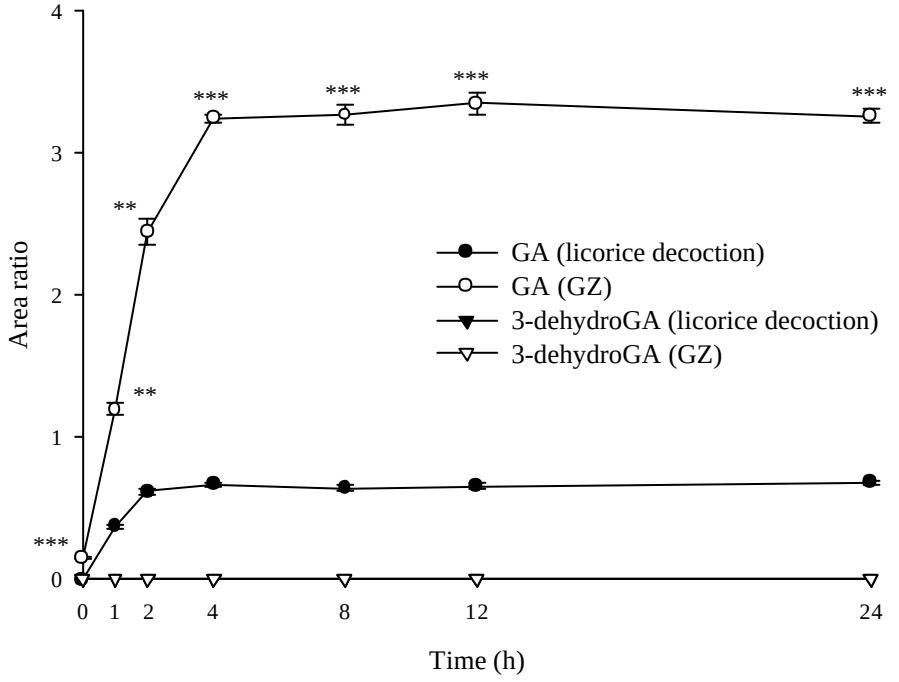

Fig. 42. Mean (± S.D.) peak area ratio-time profiles of GA and 3-dehydroGA after incubation of glycyrrhizin or licorice decoction with human feces (n=3).

* $p < 0.05$, ** $p < 0.01$, *** $p < 0.001$ compared with licorice decoction.

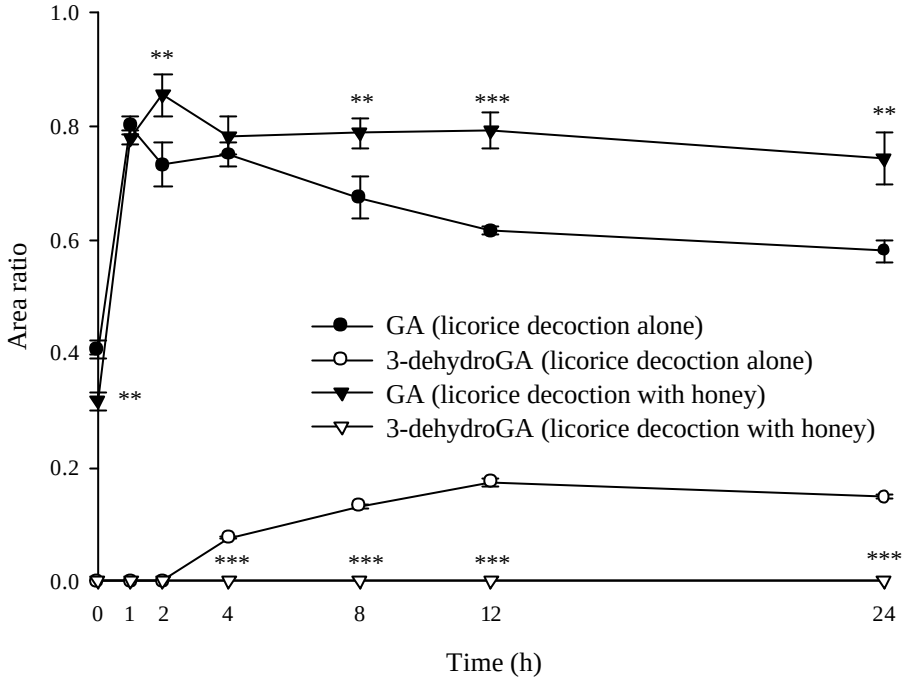

Fig. 43. Mean (± S.D.) peak area ratio-time profiles of GA and 3-dehydroGA after incubation of licorice decoction (containing 100 μg/mL GZ) alone or with honey (10 mg/mL) in rat feces (n=3).

* $p < 0.05$, ** $p < 0.01$, *** $p < 0.001$ compared with licorice decoction alone.

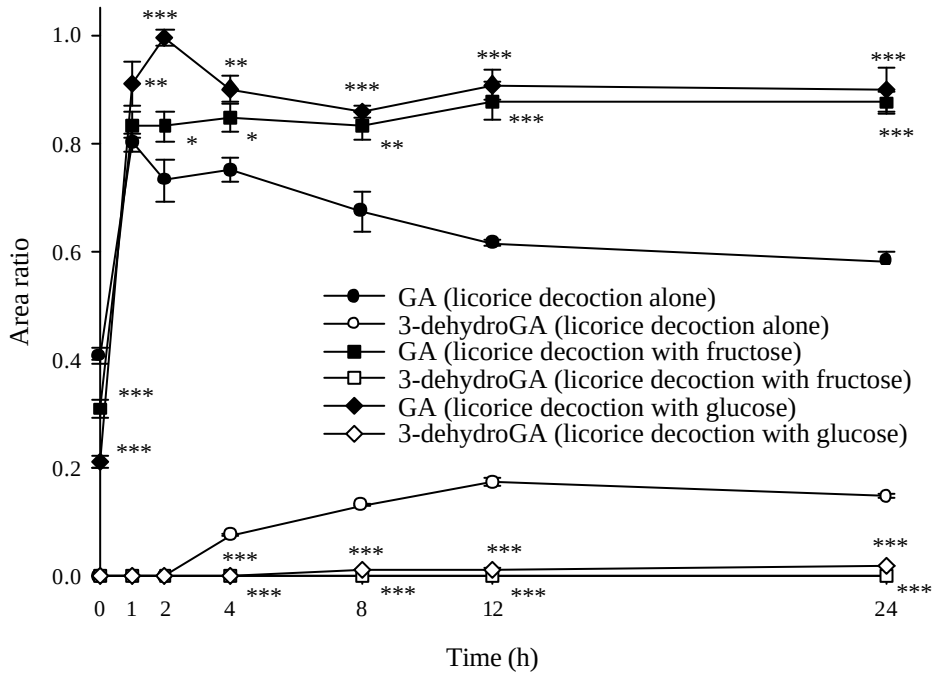

Fig. 44. Mean (± S.D.) peak area ratio-time profiles of GA and 3-dehydroGA after incubation of licorice decoction (containing 100 μg/mL GZ) alone and with fructose or glucose (10 mg/mL) in rat feces (n=3).

* $p < 0.05$, ** $p < 0.01$, *** $p < 0.001$ compared with licorice decoction alone.